OPTIMAL SHAPE OF A DISTRIBUTED RC NOTCH FILTER - A COMPUTER-AIDED DESIGN

OPTIMAL SHAPE OF A DISTRIBUTED RC NOTCH FILTER - A COMPUTER-AIDED DESIGN

by

JOHN D. KOSTYNYK, B. ENG.

A Thesis

Submitted to the School of Graduate Studies

in Partial Fulfilment of the Requirements

for the Degree

Master of Engineering

McMaster University

April 1972

MASTER OF ENGINEERING (1972)
(Electrical Engineering)

McMASTER UNIVERSITY
Hamilton, Ontario

TITLE: "Optimal Shape of a Distributed RC Notch Filter"

AUTHOR: John D. Kostynyk, B. Eng. (McMaster University)

SUPERVISOR: Professor C. K. Campbell

NUMBER OF PAGES: ix, 93.

SCOPE AND CONTENTS:

A computer-aided design objective is formulated with the aim of obtaining the optimal shape of a distributed RC notch filter, where optimality is governed by the bandwidth rejection ratio and maximum attenuation. The optimized results are tabulated, and notch responses are compared with previously designed distributed RC notch filters. Models of the proposed circuits are constructed, and notch responses are compared. Dielectric losses are also considered in accounting for experimental results.

ACKNOWLEDGEMENTS

The author wishes to extend his appreciation to Dr. C. K. Campbell for his interest and guidance during this project.

The author is also extremely grateful for the ideas gained through discussions and advice from Dr. J. W. Bandler and Mr. C. Charalambous, in the field of computer-aided design. He has also benefited from discussions with Mr. E. Johnston and Mr. J. Wragg.

This project was financed through a grant-in-aid from the National Research Council of Canada to Dr. C. K. Campbell. The author is also indepted to McMaster University for financial support in the form of a McMaster Assistantship.

ABSTRACT

An improvement on the synthesis of a distributed RC notch filter, by computer-aided design techniques, is appraised. A brief presentation of the synthesis of thin-film RC tapered networks is made, along with applied uses of computer-aided design to RC distributed networks , particularly in the realizability of certain RC transfer functions.

The preparation of the problem, accompanied by different methods of approach, is explained. Included, are criticisms made, leading to the reasons for abandoning the more tasking ones.

The Adjoint Network method of determining gradients, with respect to circuit adjustable parameters, is evaluated fully, and the important use which it lends to the optimization problem is demonstrated. The outcome of the design approaches are given in tables, with theoretical responses compared in graphs. Actual circuit responses are indicated in photographs, and comparisons with theoretical responses are shown in graphs.

TABLE OF CONTENTS

LIST OF FIGURES

CHAPTER 1

INTRODUCTION

With the advent of microcircuits, it appeared that circuit theory was receiving another opportunity to show its mettle. But the method often adopted in realizing network functions, using distributed circuits, was to transform the distributed network problem in the S-plane, to an equivalent lumped one in some transformed plane[27]. Thus in the beginning, distributed networks overly forced analogies with lumped networks, thereby limiying their utility.

These limitations are manifested by interactions in the distributed network, which would adversely affect the analysis in lumped element form. For example, the behaviour of a deposited resistive layer may be degraded at high frequencies because of the proximity of a ground plane. Hence, in order that they be implemented to their greateset advantage, the elements must be analysed as distributed circuit elements, rather than lumped circuit elements.

Most important in these advantages are the considerations of device dimensions and reduced interconnections, which enhance reliability. As well, distributed circuits provide more phase shift with less attenuation, than is available with lumped element circuits. But the investigation of nonuniform shapes (or tapered structures) is even more significant because they produce even better phase shift with less attenuation narrower bandwidth rejection ratios, better dB gain, and provide differ-

ent input or output impedance levels, than is available with a uniform RC (URC) structure.

In general, nonuniform tapers could only be of the forms explained in section 4.1.1 of this thesis, (linear,exponential, or trigonometric) because of the resultant 2nd order differential equation, which is a formidable problem to solve.

But even in these cases, the transmission zeros of the open circuit voltage transfer function must lie at infinity, as demonstrated in the paper by Protonotarios[20]. Subsequently, much time and effort was expended in developing schemes to produce finite S-plane zeros. Wyndrum[27] proposed the interconnection of URC's, in ladder configurations, to give negative real-axis zeros. O'Shea[18] then expanded this thought, to parallel networks, and lattice configurations, which enabled the transfer function zeros to lie anywhere in the S-plane. But the cost, and reliability of so many interconnections had definite drawbacks, and realization of the circuits was impractical.

As was investigated by O'Shea, the interconnection of many URC's enabled the complex transmission zeros to lie anywhere in the complex S-plane. Heizer[10] not only presented a multilayer RC (MRC) structure, which incorporated this thought, but he also set forth a method of rational transfer synthesis from distributed RC networks. Note that previous distributed networks, had transfer functions which were irrational functions of frequency, while present methods of design are based on rational transfer functions.

But the restrictions on Heizer's circuits are weighty. The need that the resistive taper be uniform, and that the sum of the capacitance

and conductance tapers also be uniform, greatly limits the choice of pole locations. There was also great difficulties encountered in the construction of his circuits - thus the lack of experimental verification!

Probably the most exemplary technique which applied an iterative scheme to obtain a realizable transfer function from a readily constructed circuit, was that proposed by Walsh and Close[25]. They used the same basic structure as Heizer, but reversed the input and output ports (see figure 1.1).

They then proceeded to obtain a resistance taper, by an iteration method proposed by Newton , which then yielded the desired pole locations of the network transfer function. Following this the capacitance and conductance tapers were determined by a similar method, which realized the desired transmission zeros, and made the transfer function rational. The end result was that all zeros could be freely chosen, and the poles could all be distinct, and lie and the negative real axis.

They then made modifications to the realized tapers, to accomodate: (a) the case where the capacitance was negative for part of the line, and (b) the fact that the circuit, if it were to be constructed of homogeneous material of uniform thickness, then the RC product must be made constant along the line.

The method, although it was good for realizing required poles and zeros, it was quite cumbersome and involved mathematically before any computer iterative scheme was used. Also the final results were not as promising as expected for a computer-aided design. But it may be quite an adaptable method for cases where very general responses are desired and the system transfer function is readily obtainable.

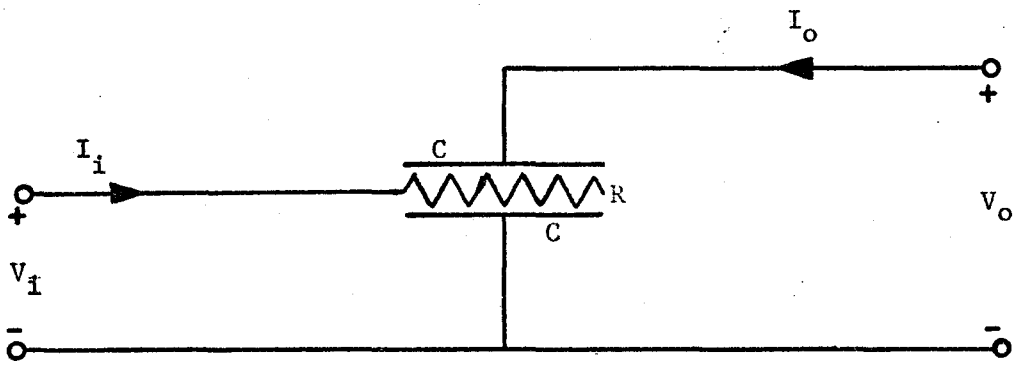

(a) Heizer's basic circuit.

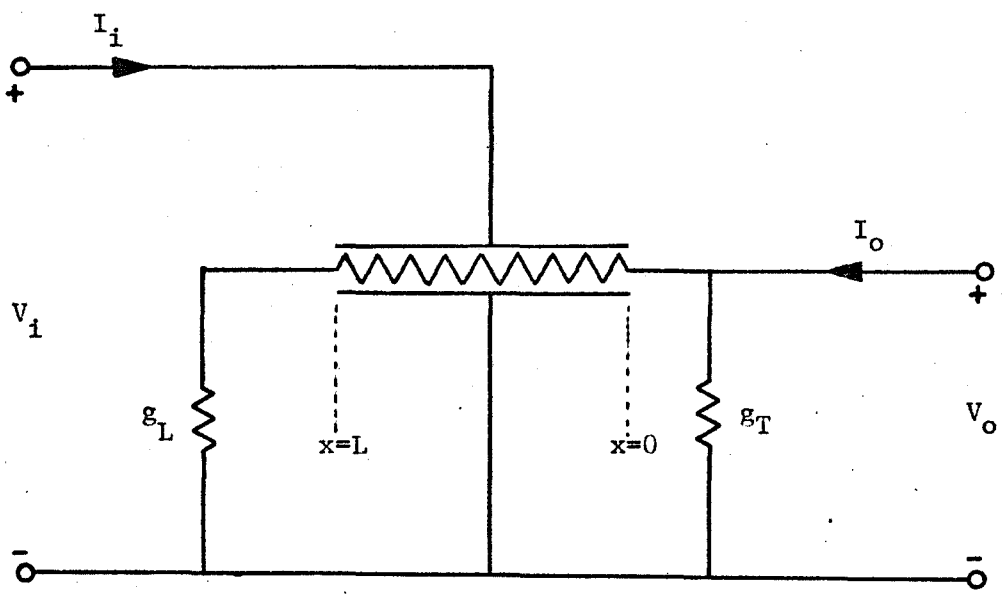

(b) Circuit of Walsh and Close.

Figure 1.1

Schematic representation of circuits utilized by (a) Heizer, and (b) Walsh and Close.

In all previous instances, it must be the designers burden to synthesize a real circuit, according to some specified response requirements - whether the design employs computer-aided design methods, or not. Once some initial design is constructed, a test must be made to ascertain the quality of the circuit response, relative to the desired response. In all probability, some intuitive adjustment of circuit parameters is necessary, in order to improve this quality.

So in most engineering endeavours, it becomes necessary to design, sample and redesign, where a computer facility may relieve the design engineer of much tedium and unnecessary "drudgery". That is, unless of course, the circuit may be designed by computer-aided design techniques alone. Thus if limitations are acknowledged, and a "proper design criterion is established, the best possible parameters that will yield the "best" quality, may be contracted.

It will be the task of this thesis, to investigate why, and how a computer-aided design method may be applied to obtain the optimal shape of a thin-film RC structure, which will yield the "best" notch response. The criteria of "best" notch response are with respect to the bandwidth rejection ratio, and the greatest obtainable attenuation. Theoretical responses of the proposed structures will be compared with theoretical responses of other networks already known to have good bandwidth rejection ratios.

The comparative, and optimal model thin-film circuits will be constructed to ascertain the validity of certain assumptions, and to

compare the optimally designed network response, with previously designed ones. Theoretical calculations of the notch frequency will also be performed and discrepancies will be clarified.

CHAPTER 2

REVIEW OF DISTRIBUTED RC NETWORK ANALYSIS

2.1 General Two-Dimensional Diffusion Equation

The physical structure of a thin-film or distributed-parameter RC network is shown in figure 2.1. In general, it is planar and constructed of homogeneous materials of constant thickness. This thickness is assumed to be infinitesimal so that the resistance and capacitance per unit length, are functions of width only, and current flow is essentially two-dimensional.

The most general fundamental equation which describes the behaviour of a two-dimensional distributed RC network, can be derived by considering an incremental section of the network as in figure 2.2.

If some time-varying voltage is applied at port 1, then there will be an electric field developed in the resistive layer. If R(x,y) is the resistance per unit square, then this electric field is given by :

$$\underset{\sim}{E}(x,y,t) = R(x,y) \; \underset{\sim}{J}(x,y,t) \qquad (2.1)$$

where J(x,y,t) is the current density at some position (x,y).

Governed by the basic law that electric charge must be conserved, and preserved in the form of the divergence theorem, the divergence of the conduction current in an incremental element of the resistive layer is equal to the displacement current-flow out of an incremental element of capacitance. More descriptively,

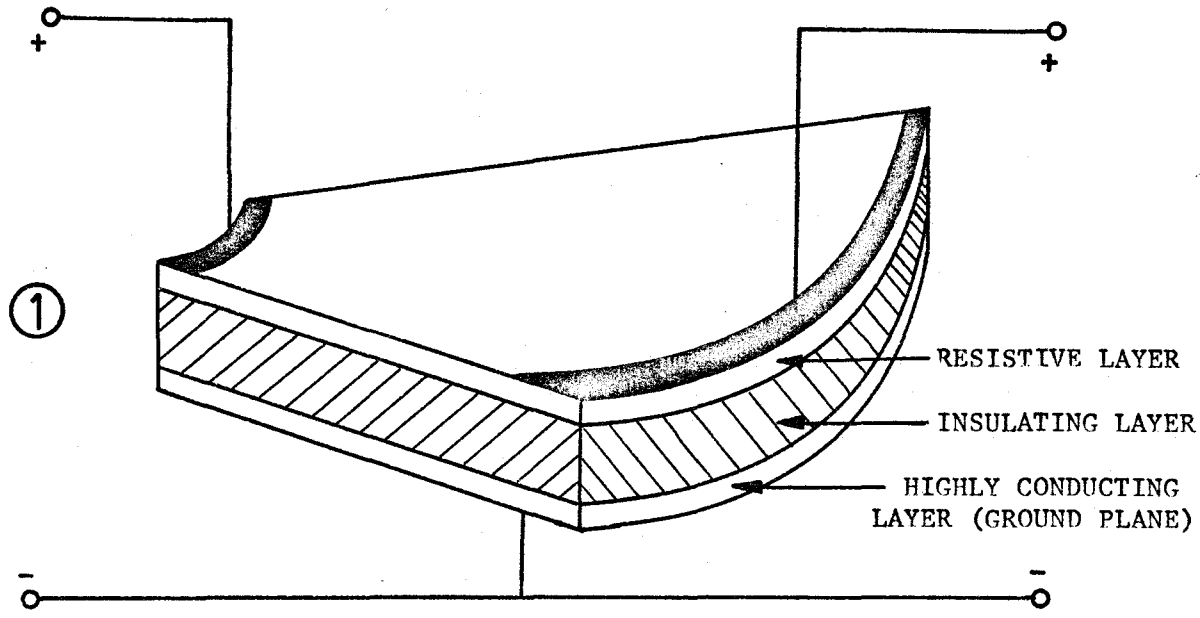

Figure 2.1

Physical structure
of distributed RC circuit showing two-dimensional current flow.

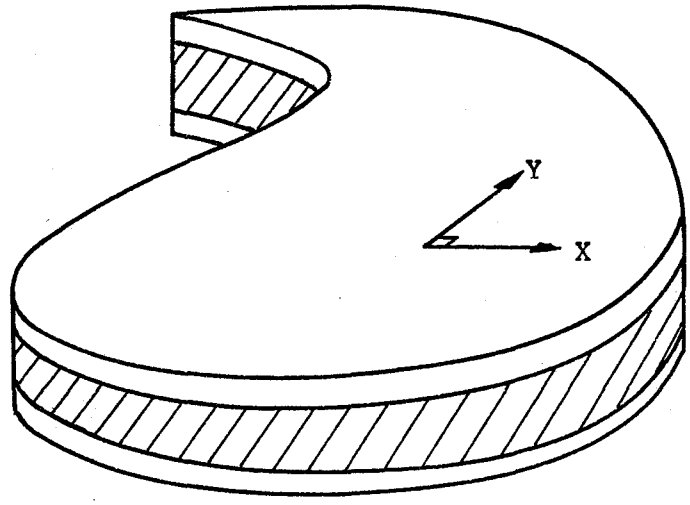

Figure 2.2

Any general small element from the structure of fig. 2.1

$$\nabla \cdot \underset{\sim}{J}(x,y,t) = -C(x,y) \frac{\partial V(x,y,t)}{\partial t} \tag{2.2}$$

where C(x,y) is the capacitance per unit area between the conducting planes, and V(x,y,t) is the potential of a point in the resistive layer with respect to the ground plane.

Typical values of structure resistance and capacitance are such, that inductance effects can be assumed to be negligible, and hence are ignored for purposes of this analysis. This may also be justified in that the experimental results agree closely with theoretical predictions. Thus the electric field may be written as

$$E(x,y,t) = -\nabla V(x,y,t) \tag{2.3}$$

This substitution into equation (2.1) will yield

$$\frac{-\nabla V(x,y,t)}{R(x,y)} = \underset{\sim}{J}(x,y,t) \tag{2.4}$$

and since the divergence of equation (2.4) is

$$-\nabla \cdot \left\{ \frac{\nabla V(x,y,t)}{R(x,y)} \right\} = \nabla \cdot \underset{\sim}{J}(x,y,t) \tag{2.5}$$

the results of equation (2.2), when combined with equation (2.5) give

$$\nabla \cdot \left\{ \frac{\nabla V(x,y,t)}{R(x,y)} \right\} = C(x,y) \frac{\partial V(x,y,t)}{\partial t} \tag{2.6}$$

If R(x,y) and C(x,y) are constant with regard to the location in the distributed network, equation (2.6) reduces to

$$\nabla^2 V(x,y,t) = RC \frac{\partial V(x,y,t)}{\partial t} \qquad (2.7)$$

The Laplace Transform recasts equation (2.7) (for zero initial conditions)

$$\nabla^2 V(x,y,s) = sRC\ V(x,y,s) \qquad (2.8)$$

Now for purely notational purposes, if we let $\bar{V}(x,y)$ represent $V(x,y,s)$ and give it the properties of a function of position and a phasor function in time, then equation (2.8) reduces finally to

$$\nabla^2 \bar{V}(x,y) = sRC\ \bar{V}(x,y) \qquad (2.9)$$

which is a form of the familiar diffusion equation.

It is the exact solution of this equation we are interested in for any two-dimensional thin-film RC network. This solution yields the voltage and current, and immittance dependencies, on the two-dimensional properties of the network. If attention is restricted to one-dimensional current flow (as in some approximation methods), then the introduction of a taper results in resistance per unit length and capacitance per unit length, which are functions of position along the direction in which current flows. At best, only a rough approximation! Further comment will be reserved for Chapter 4.

2.2 Uniformly Distributed RC (URC) Structure

The basic construction of a URC network is similar to the general one shown in figure 2.1, but for the fact that the conducting contacts at either end of the resistive layer, are now physically para-

llel to each other, as in figure 2.3. Thus the current flow will be strictly in one direction, and there will be no current differential developed across the width (y-axis) of the structure. The structure may now be analysed as a uniformly distributed RC transmission line. A schematic representation of this structure is shown in figure 2.4.

The open circuit low-pass response of this circuit may be determined by examining an equivalent circuit showing an incremental section, as depicted in figure 2.5. Here the conducting layer is assumed to have zero resistance, and the dielectric is lossless.

From Kirchoff's voltage and current description of the circuit one obtains

$$v(t,x) = r_o \Delta x \cdot i(t,x) + v(t,x+\Delta x) \tag{2.10}$$

$$i(t,x+\Delta x) - i(t,x) = -c_o \Delta x \cdot \frac{\partial v(t,x+\Delta x)}{\partial t} \tag{2.11}$$

where

r_o = resistance per unit length

c_o = capacitance per unit length

If the initial conditions are assumed to be zero, then by allowing $\Delta x \rightarrow 0$ in equations (2.10) and (2.11), and taking the Laplace Transform of the resultant partial differential equation

$$\frac{dV(s,x)}{dx} = -r_o \cdot I(s,x) \tag{2.12}$$

$$\frac{dI(s,x)}{dx} = -sc_o \cdot V(s,x) \tag{2.13}$$

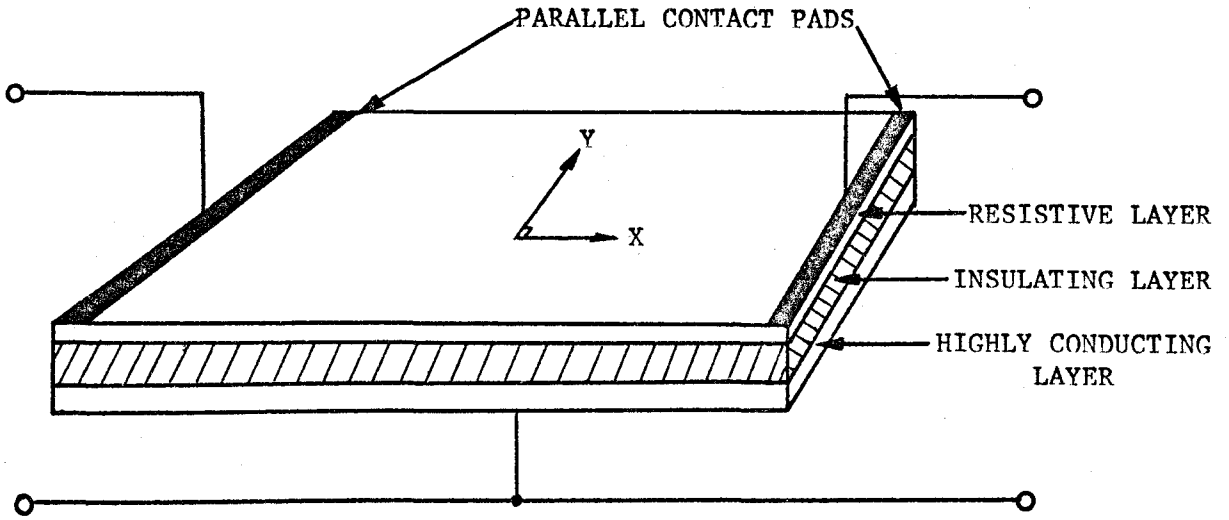

Figure 2.3

Physical structure of URC circuit.

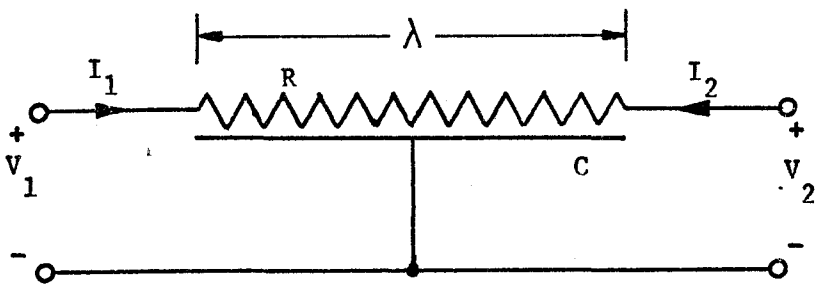

Figure 2.4

Equivalent circuit representation of URC structure.

If, equation (2.12) is then differentiated, and a substitute for $\frac{dI(s,x)}{dx}$ from equation (2.13) is made, a 2nd order differential equation of the form

$$\frac{d^2V(s,x)}{dx^2} - sr_oc_oV(s,x) = 0 \tag{2.14}$$

is obtained. A similar operation on equation (2.13) yields

$$\frac{d^2I(s,x)}{dx^2} - sr_oc_oI(s,x) = 0 \tag{2.15}$$

The solution to equation (2.14) is then

$$V(s,x) = Ae^{\beta x} + Ce^{-\beta x} \tag{2.16}$$

where

β(propagation function) $= \sqrt{sr_oc_o}$

If boundary conditions such as those shown in figure 2.5 are imposed; in other words

$$\begin{aligned} V_1 &= V(s,0) & V_2 &= V(s,\lambda) \\ I_1 &= I(s,0) & I_2 &= -I(s,\lambda) \end{aligned} \tag{2.17}$$

the y-parameters for the overall network may be extracted, as

$$y_{11} = y_{22} = \frac{1}{Z_o}\coth\Theta \tag{2.18}$$

$$y_{21} = y_{12} = -\frac{1}{Z_o}\operatorname{csch}\Theta \tag{2.19}$$

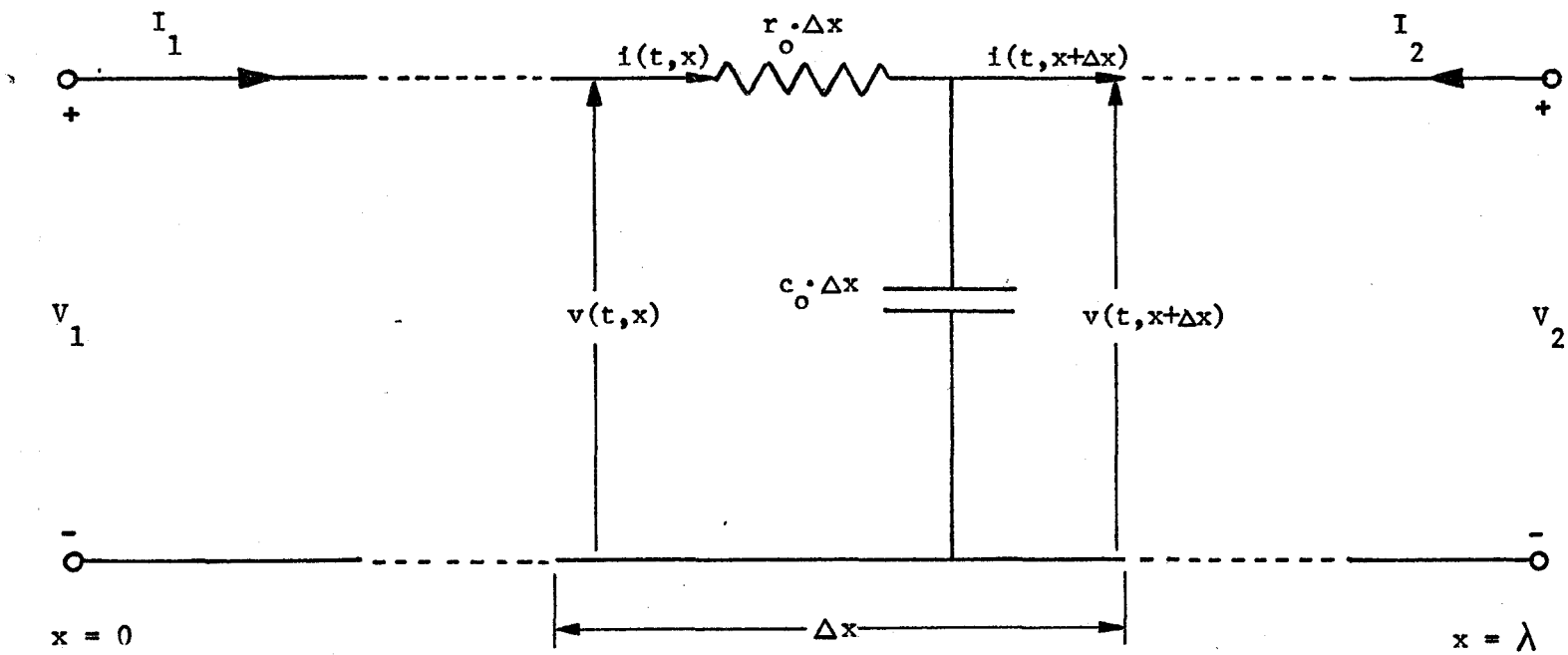

Figure 2.5

Incremental element model (length Δx) of the distributed RC circuit.

where

$$\Theta = \sqrt{sr_o c_o \lambda^2} = \sqrt{sRC}$$

$$Z_o = \sqrt{\frac{r_o}{sc_o}} = \sqrt{\frac{R}{sC}}$$

λ = overall length of the structure

$R = r_o \lambda$ = total series resistance of structure

$C = c_o \lambda$ = total capacitance of structure

The ABCD-parameter and z-parameter description of the network can also be obtained, by the appropriate conversion operation on equations (2.18) and (2.19). Thus the open circuit voltage transfer function becomes

$$T = \left.\frac{V_2}{V_1}\right|_{I_2=0} = -\frac{y_{21}}{y_{22}} = \frac{1}{\cosh \Theta} \tag{2.20}$$

The poles of T may be determined by substituting the product expansion of $\cosh\Theta$, as

$$\cosh\Theta = \prod_{n=1} \left\{1 + \frac{4\Theta^2}{(2n-1)^2\pi^2}\right\} \tag{2.21}$$

into equation (2.20). The result being that equation (2.20) is an all pole function; the poles located at

$$s = -\frac{(2n-1)^2 \pi^2 \omega_o}{4} \qquad n = 1,2,3,\ldots \tag{2.22}$$

where

$$\omega_o = \frac{1}{RC}$$

2.3 URC Structure As Notch Filter

In order that a notch filter response be obtained from a simple URC low pass filter, the open circuit voltage transfer function must contain a zero on the $j\omega$ axis . Examination of the T or Π equivalent circuits of the URC, in figures 2.6(a) and 2.6(b) respectively, will aid in the choice of the appropriate immittance element which will give this transmission zero.

For the T equivalent circuit, an impedance of $Z_T = -Z_B$ in series with Z_B : and for the Π equivalent circuit an admittance of $Y = -Y_b$ in parallel with Y_b will yield this transmission zero.

From figure 2.6, and the expressions for the y-parameters and z-parameters or the URC, we may extract the necessary immittance expressions, as,

$$Y_b = -y_{12} = \frac{\sqrt{jx}}{R\sinh\sqrt{jx}} \tag{2.23}$$

$$Z_B = z_{12} = \frac{R}{\sqrt{jx}\,\sinh\sqrt{jx}} \tag{2.24}$$

where

$$x = \omega RC$$

The necessary immittances, Z_b and Y_B may be obtained by the correct choice of R's, L's, and C's, or combinations thereof. This choice was investigated by Stein[22], and was found to be a function of x ($=\omega RC$) The combinations of these lumped elements was found to be repetitive for $x > 99.93$. Hence countless combinations of these lumped elements will give the sought after transmission zero.

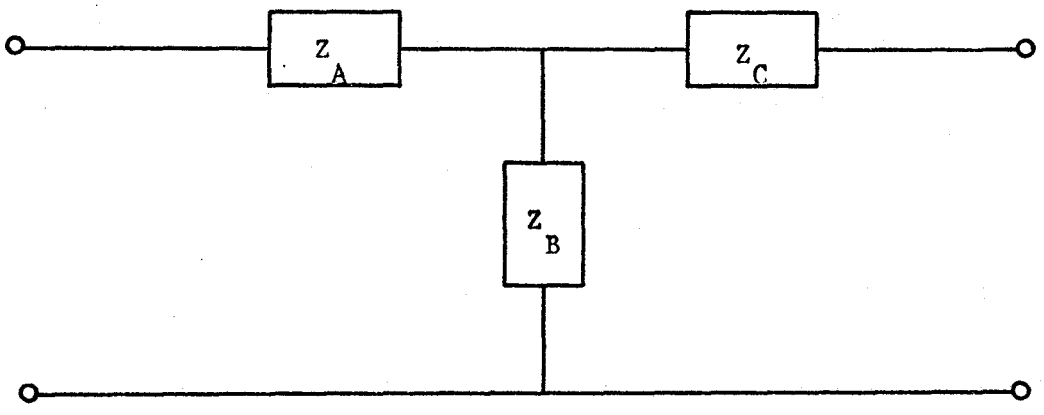

(a) T-equivalent circuit

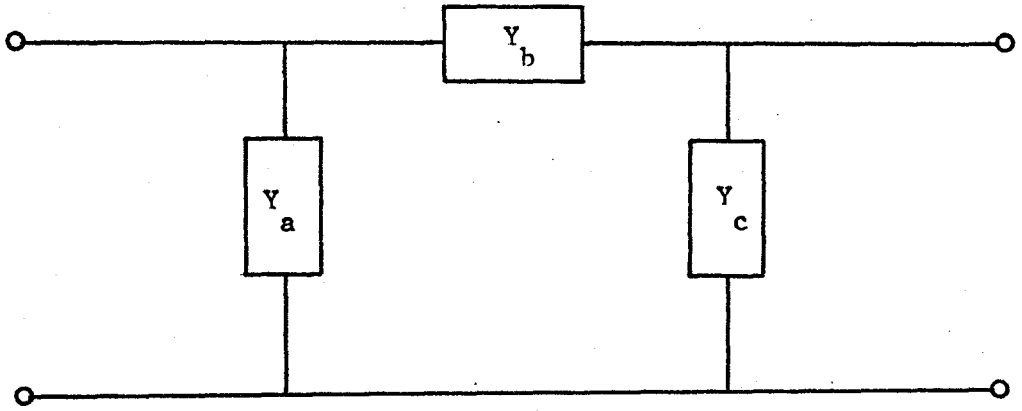

(b) Π -equivalent circuit

Figure 2.6

Π - and T-equivalent circuit of the URC structure.

A resistor in series with the T network is the lumped element chosen, for several reasons: ease of fabrication, minimal size, most easily varied, it can be trimmed by laser to a high degree of tolerance, and it costs the least.

The resultant network - URC in series-series with a lumped resistor - is depicted in figure 2.7. Since they are so simply connected - series - the z-parameters of each element (lumped and distributed) may be added to obtain the z-parameters of the overall network. So that

$$z_{11} = z_{22} = \frac{R}{\Theta}\coth\Theta + R_N \tag{2.25}$$

$$z_{12} = z_{21} = \frac{R}{\Theta}\operatorname{csch}\Theta + R_N \tag{2.26}$$

Thus the open circuit transfer function may be obtained as

$$T = \left.\frac{V_2}{V_1}\right|_{I_2=0} = \frac{\alpha + \Theta\sinh\Theta}{\alpha\cosh\Theta + \Theta\sinh\Theta} \tag{2.27}$$

where

$$\alpha\,(\text{notch parameter}) = \frac{R}{R_N}$$

$$\Theta = \sqrt{jx}$$

$$x = \omega RC$$

Only if the numerator of T equals zero, will there be a zero of transmission. In other words,

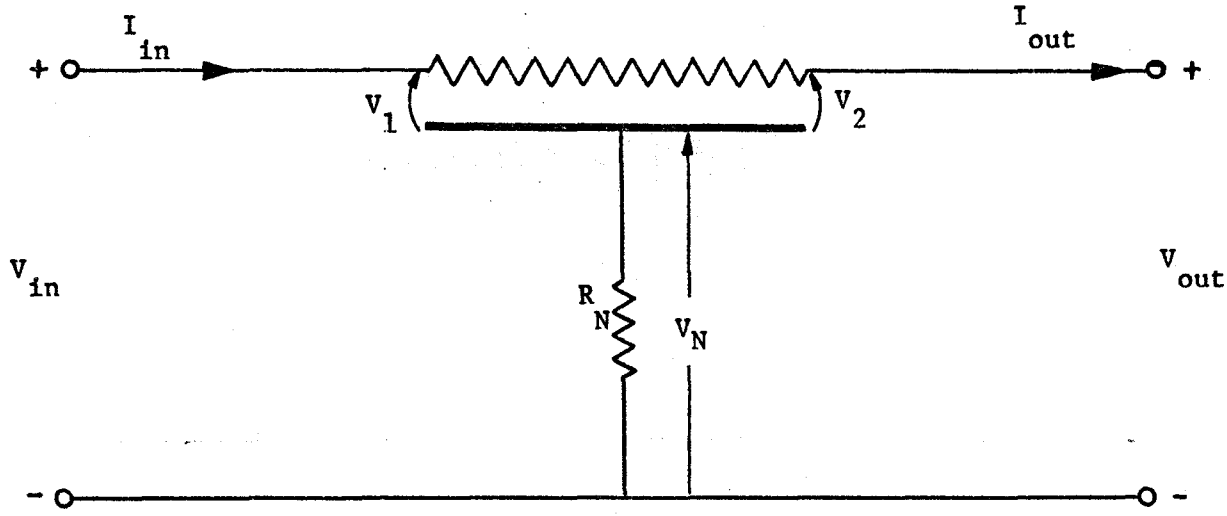

Figure 2.7

URC notch filter.

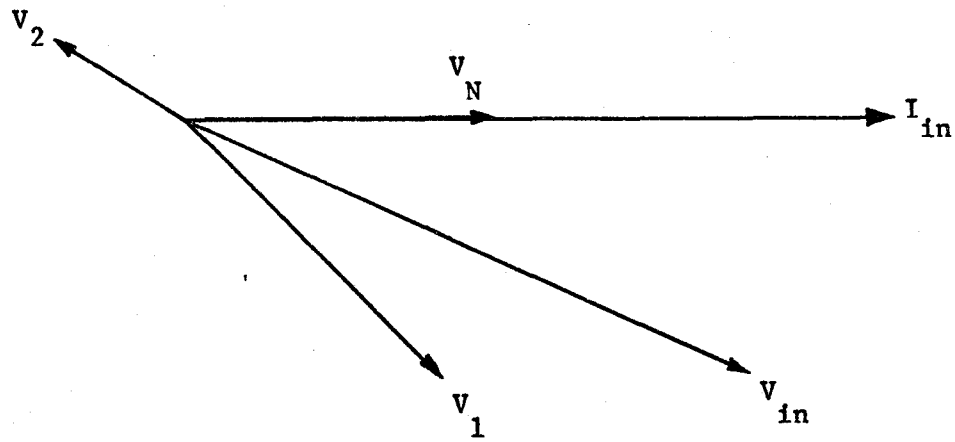

Figure 2.8

Phasor diagram of URC notch filter

$$\alpha + \sqrt{jx}\,\sinh\sqrt{jx} = 0 \tag{2.28}$$

or

$$\alpha + \frac{1+j}{2}\,x^{\frac{1}{2}}\,\sinh\left(\frac{1+j}{2}\,x^{\frac{1}{2}}\right) = 0 \tag{2.29}$$

By using the identity of equation (2.30), below), in equation (2.29)

$$\sinh(a + jb) = \sinh(a)\cos(b) + j\cosh(a)\sin(b) \tag{2.30}$$

and equating the resultant imaginary part to zero, the following transcendental function is obtained

$$\tanh(y) = -\tan(y) \tag{2.31}$$

where

$$y = \sqrt{\frac{x}{2}}$$

The frequency at which the null occurs, may be found by solving equation (2.31) as a function of y. In doing this, the points of intersection of the hyperbolic and trigonometric functions, and hence the solution to the equation, is found to be

$$y_n = n\pi - \frac{\pi}{4} \qquad n = 1,2,3,\ldots \tag{2.32}$$

Hence a null may occur at an infinite number of frequencies, since

$$y_n = \sqrt{\frac{x_n}{2}} = \sqrt{\frac{2\pi f_n RC}{2}} \tag{2.33}$$

Table 2.1

Values of notch parameter (α), and x (= ωRC) for different values of n

n	x_n	α_n
1	11.1902	17.786
2	60.451	-949.161
3	149.278	3.45×10^4
4	277.583	-1.089×10^6
5	445.366	3.1924×10^7

Then α may be found from the resultant real part of substituting the identity, equation (2.30), into equation (2.29), and equating this to zero to yield

$$\alpha = 2\sqrt{\frac{x}{2}} \sin\sqrt{\frac{x}{2}} \cosh\sqrt{\frac{x}{2}} \tag{2.34}$$

Table 2.1 indicates the values of α and x, for several values of n. But in practice only values of n which give a positive α (in other words, for n odd), will be considered.

2.4 Physical Operation of Notch Filter

Figure 2.7 provides an excellent reference diagram for determining the vector equations and phasor diagram, and enhances the physical operation of the URC notch filter.

Since all the input current, (I_{in}), flows through the notch resistor and URC structure, in the open circuit transfer function configuration, it is a good reference phasor for the other voltages and currents.

Because of the open circuit load, the input voltage (V_{in}) propogates the length of the structure, and is reflected from the output port, But only in partial truth, for due to severe attenuations in the structure, the reflected wave, on its return to the input, is so insignificant it may be ignored. The consequences being that, effectively,

$$\underset{\sim}{V}_{in} = Z_o \underset{\sim}{I}_{in} \tag{2.35}$$

where

$$Z_o \text{ (characteristic impedance)} = \sqrt{\frac{R}{sC}}$$

Since the input current flows through the notch resistor, the voltage across the notch resistor (V_N) is in phase with this current, as in figure 2.8. And

$$\underset{\sim}{V}_N = \underset{\sim}{I}_{in} R_N \tag{2.36}$$

Due to the capacitive-resistive impedance nature of the URC structure, the voltage at the input of this structure (V_1) lags the input current (I_{in}) by 45^o. Now the input voltage to the notch network (V_{in}), is the vector sum of the input voltage at the URC structure, and the voltage across the notch resistor, namely

$$\underset{\sim}{V}_{in} = \underset{\sim}{V}_1 + \underset{\sim}{V}_N \tag{2.37}$$

Also, the output voltage (V_{out}) of the notch network, is the vector sum of the voltage across the notch resistor, and the attenuated voltage (V_2) at the output of the URC structure.

$$\underset{\sim}{V}_{out} = \underset{\sim}{V}_2 + \underset{\sim}{V}_N \tag{2.38}$$

From this description of the voltage vectors, if the open circuit voltage transfer function is written as

$$T = \left.\frac{\underset{\sim}{V}_{out}}{\underset{\sim}{V}_{in}}\right|_{\underset{\sim}{I}_{out} = 0} = \frac{\underset{\sim}{V}_2 + \underset{\sim}{V}_N}{\underset{\sim}{V}_1 + \underset{\sim}{V}_N} \tag{2.39}$$

then a zero of transmission, and thus a null, will occur when $\underset{\sim}{V}_2$ and $\underset{\sim}{V}_N$ are equal and opposite in phase. For the condition of notch parameter and frequency at which this null occurs, a more descriptive analysis is given in a paper by Campbell[4].

A typical URC notch network response is given in figure 2.9, where the frequency is normalized with respect to f_o (= $1/2\pi$RC). Note the notch responses for values of α, which do not yield a zero of transmission in equation (2.27) - α = 10, and α = 30.

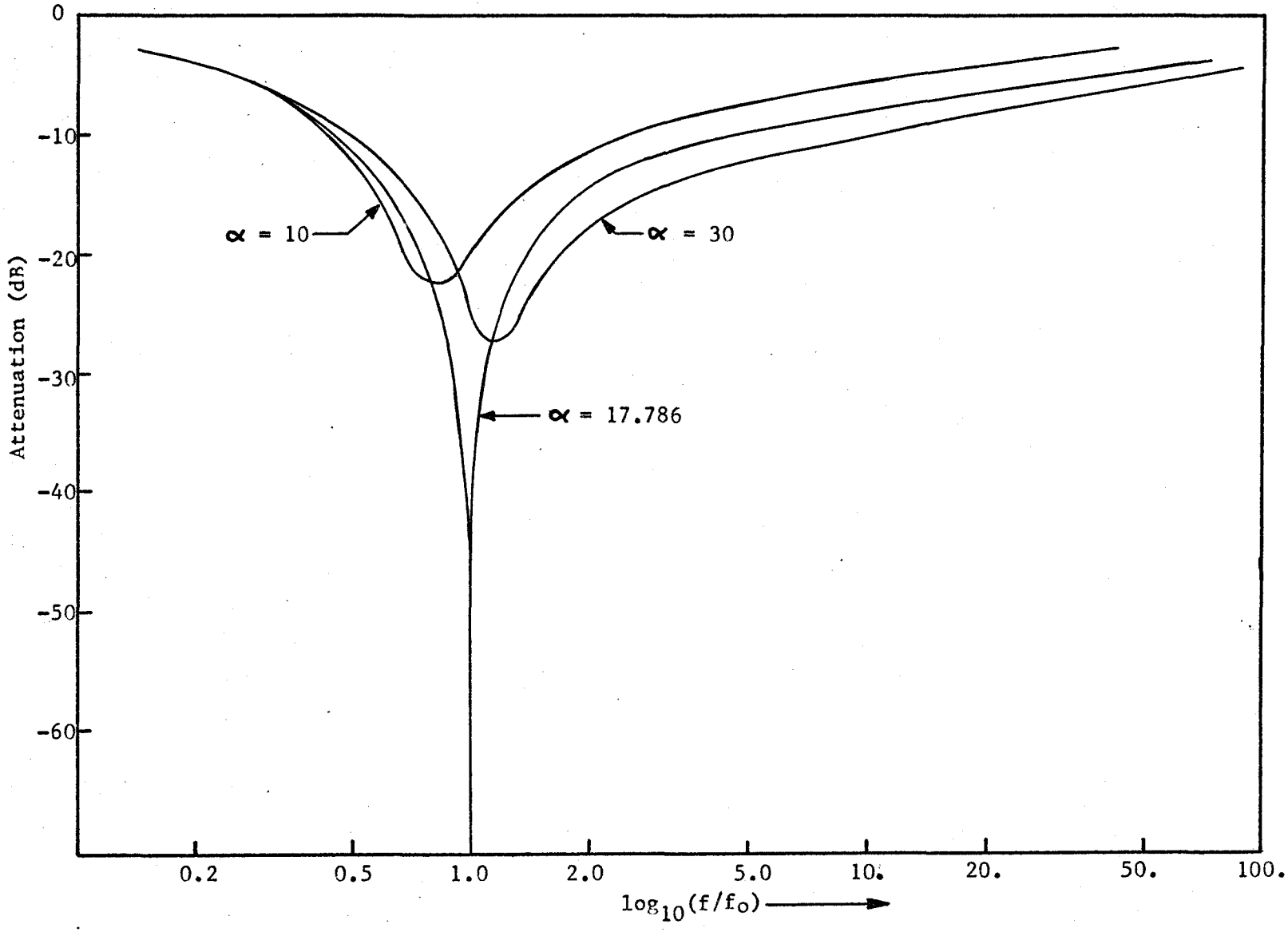

Figure 2.9

Comparison of notch responses for URC notch network, for optimal and non-optimal α.

CHAPTER 3

COMPUTER-AIDED DESIGN

3.1 General Philosophy

As mentioned, one's quest for a design solution invariably leads through a sequence of progressive steps, with a generak feedback of information, so that the "best" possible circuit configuration may be formulated. In all cases a firm understanding of physical principles is vital, so that interpretation of results gives an accurate picture of the relative merits of each design consideration. Hence the optimization techniques are generally tools, which may be applied to improve these designs. They may not replace one's intuitive insights, or the inventiveness of a designer.

A superficial understanding of computer-aided design methods may be gleaned from the following simple concepts. A more complete understanding is presented in the reference to Bandler[1] .

3.2 Basic Concepts

Fundamentally, the primary concern is to extremize a performance measure or scalar objective function, U, where

$$U \triangleq U(\underset{\sim}{\phi}) \tag{3.1}$$

and $\underset{\sim}{\phi}$ is a vector of m independent adjustable parameters. This performance measure is a gauge of what is "best" when all the constraints of the

system are applied to the problem.

The parameters, $\underset{\sim}{\phi}$, are the ones of the system which are generally restricted to operate within some limitations. These limitations are usually incoroprated into the problem, customarily by way of constraints. The constraining relationships are closely related to the performance measure, and often contained in it.

The more prevalent relationships inhibiting $\underset{\sim}{\phi}$, are those of inequality constraints, exhibited by the following vector equation;

$$\underset{\sim}{g}(\underset{\sim}{\phi}) = \left[g_1(\underset{\sim}{\phi}) \quad g_2(\underset{\sim}{\phi}) \ldots\ldots \quad g_m(\underset{\sim}{\phi})\right]^T \geq \underset{\sim}{0} \tag{3.2}$$

and equality constraints of the form;

$$\underset{\sim}{h}(\underset{\sim}{\phi}) = \left[h_1(\underset{\sim}{\phi}) \quad h_2(\underset{\sim}{\phi}) \ldots\ldots \quad h_m(\underset{\sim}{\phi})\right]^T = \underset{\sim}{0} \tag{3.3}$$

A characteristic exhibited by both constraining relationships, is the necessity that they lie in some acceptable or feasible region R. Where R may be defined by any $\underset{\sim}{\phi}$, such that;

$$R \triangleq \left\{\underset{\sim}{\phi} \mid \underset{\sim}{g}(\underset{\sim}{\phi}) \geq \underset{\sim}{0},\ \underset{\sim}{h}(\underset{\sim}{\phi}) = \underset{\sim}{0}\right\} \tag{3.4}$$

and it may be assumed that $U(\underset{\sim}{\phi})$ is calculable or measurable for any $\underset{\sim}{\phi} \in R$.

A feeling for these concepts may be grasped from figure 3.2. Also included in this mapping are other optimization notations, particularly those of local (relative) minimum, which may be a minimal performance measure close to, but not absolutely, the best; and a global (absolute) minimum, which is the best.

For all the occurrences where computer-aided design may be applied, the most frequently occurring one in electrical engineering

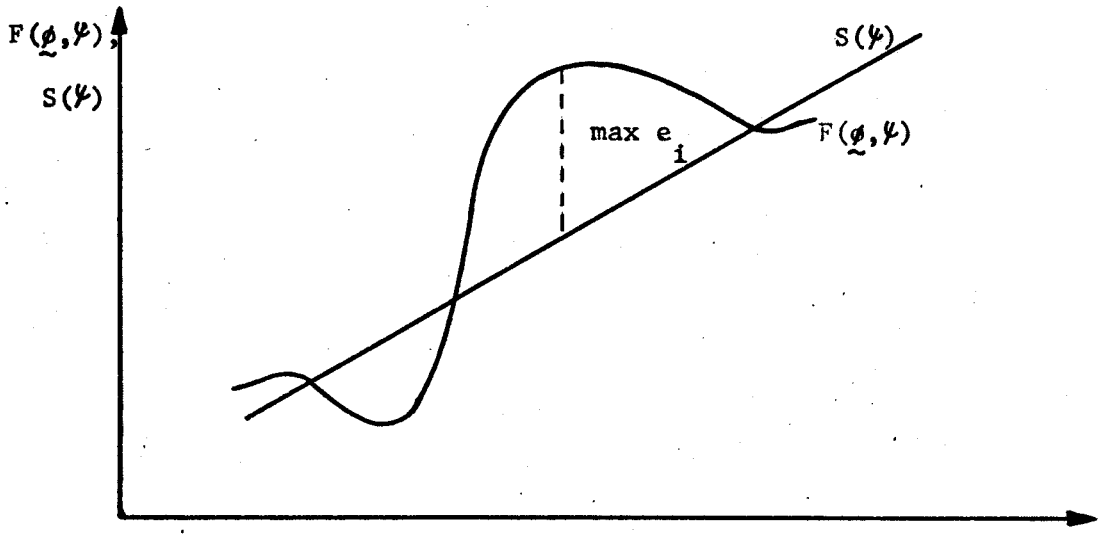

Figure 3.1

Comparison of some approximating function $F(\underset{\sim}{\phi},\psi)$ with a specified response $S(\psi)$.

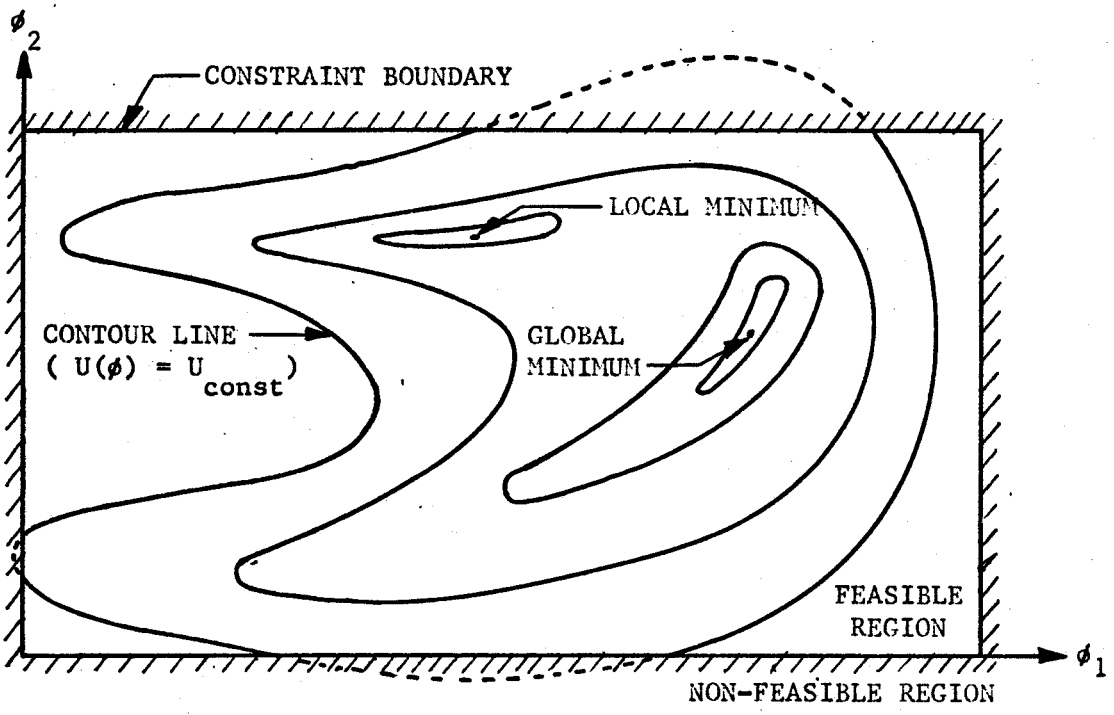

Figure 3.2

Two-dimensional contour sketch showing some features of optimization problems.

is in attempting to force some approximating function $F(\underset{\sim}{\phi},\psi)$ to have the form of some desired response $S(\psi)$, as in figure 3.1. By varying the network parameters in an optimal manner, it would become possible to reduce the errors;

$$e_i(\underset{\sim}{\phi}) = w(\psi_i)\left\{F(\underset{\sim}{\phi},\psi_i) - S(\psi_i)\right\} \tag{3.5}$$

where

$F(\underset{\sim}{\phi},\psi_i)$	is an approximating function (real or complex)
$S(\psi_i)$	is a specified response (real or complex)
$w(\psi_i)$	is a weighting function
$\underset{\sim}{\phi}$	represents circuit adjustable parameters
ψ_i	represents the i^{th} independent variable

thus forcing $F(\underset{\sim}{\phi},\psi)$ to more closely approximate $S(\psi)$.

Hence, when applying computer-aided design methods to this problem, the performance measure becomes

$$\min \; U = \sum_i \left|e_i(\underset{\sim}{\phi})\right|^p \qquad i \in I \tag{3.6}$$

where I is an index set, relating the discrete values ψ. As p becomes larger, there is more emphasis placed on larger errors, and the effect is to minimize the largest deviations.

Possibly now some disparitites of optimization methods become more physically apparent. For if an optimum exists for some $w(\psi)$ and/or p, then a different optimum will result if $w(\psi)$, or p, or both, are changed.

3.3 Choosing Computer-aided Design

3.3.1 Solving The Diffusion Equation

Having introduced computer-aided design techniques, in retrospect, one rather obvious quandary seems overlooked- "Why even consider computer-aided techniques?"

Perhaps the most necessary reason lies in the reconsideration of the diffusion equation (2.9). If the coordinate system matching the physical boundaries of the distributed circuit, belongs to a particular class of coordinate systems, then the solution of equation (2.9) may be obtained by the classical technique of "separation of variables"; where the diffusion equation in two space dimensions may be separated into two ordinary differential equations and solved by simultaneous equation method. But to pick the set of coordinate systems that is amenable to this type of solution in equation (2.9) is ponderous, since the set contains unlimited cases[18].

Methods of solving this equation become important when one wishes to gain some perspective of the relationship between electrical taper and geometrical shape. And it is precisely that type of electrical taper giving the best notch response, which we seek. In order to cover all possibilities, and determine the best taper, all cases should be tested and the one giving the "best" notch response extracted.

3.3.2 Previous Solution To Notch

As highlighted in the introduction, some authors have intuitively picked several networks and tested to see which yielded the best response [20]. Others, having challenged the optimization problem

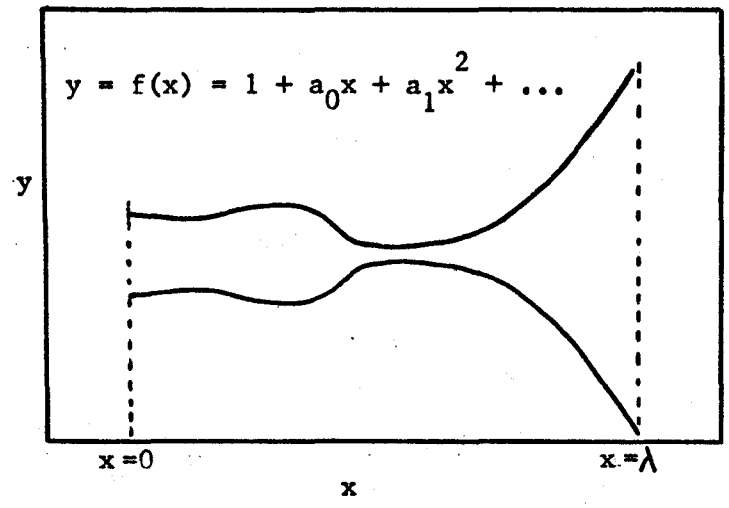

Figure 3.3

Any general shape of a thin-film RC structure.

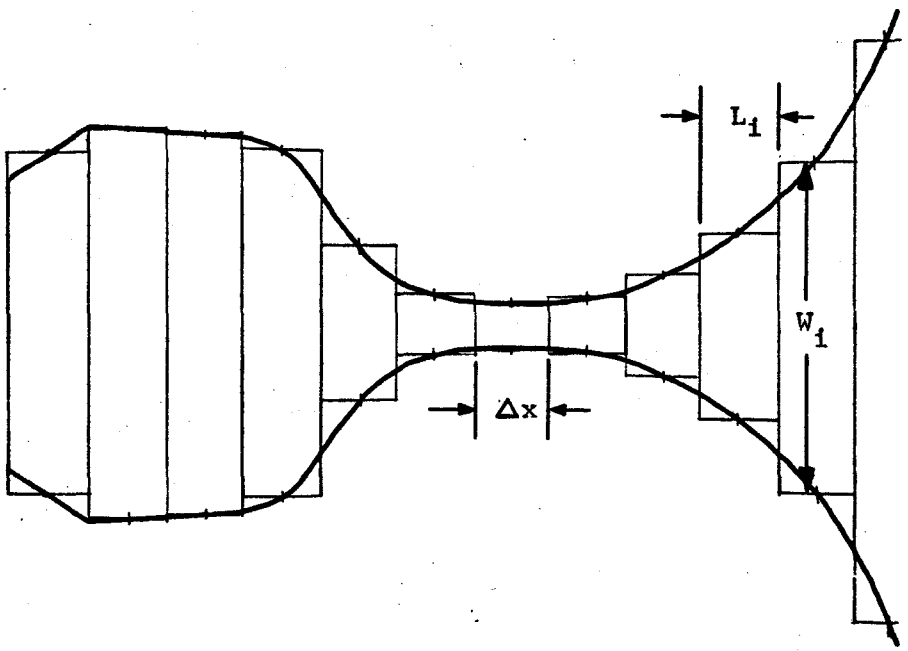

Figure 3.4

The general shape approximated by n rectangular structures, of equal length $L_i = L/n$, and width W_i.

obliquely, opted to use computer-aided techniques, but only on improving the transfer function in some optimal manner[19]. There still remained the difficulties associated with synthesizing the circuit and partially remolding the optimal function to account for circuit parameter variabilities.

As yet, none have attempted to use computer-aided design techniques to give the best direct circuit fabrication which will yield the optimal notch response. In other words, some performance measure of the notch must be minimized by varying the parameter, which must be constructed; in this case, the electrical "shape" (y - x variation) of a thin-film distributed RC network.

3.3.3. What To Optimize?

The electrical taper may be of some unexpected shape and have the functional form of a general polynomial as shown in figure 3.3.When reference is then made to figure 3.4, it's shown that any curve may be approximated if the ordinate is divided into k equal intervals Δx and the midpoints of each interval are joined. The smaller the Δx, the better the fit. Thus the shape of the thin-film RC network may be approximated by rectangular sections of length L_i and width W_i.

This would then seem to imply that a response from a tapered structure may be duplicated if the taper is closely approximated by cascading uniform RC sections.The truth lies in figure 3.5, where the notch response of an exponentially tapered RC (ERC) structure is compared with a notch response of a 25 section URC cascaded structure that approximates the exponential electrical taper - the sections being

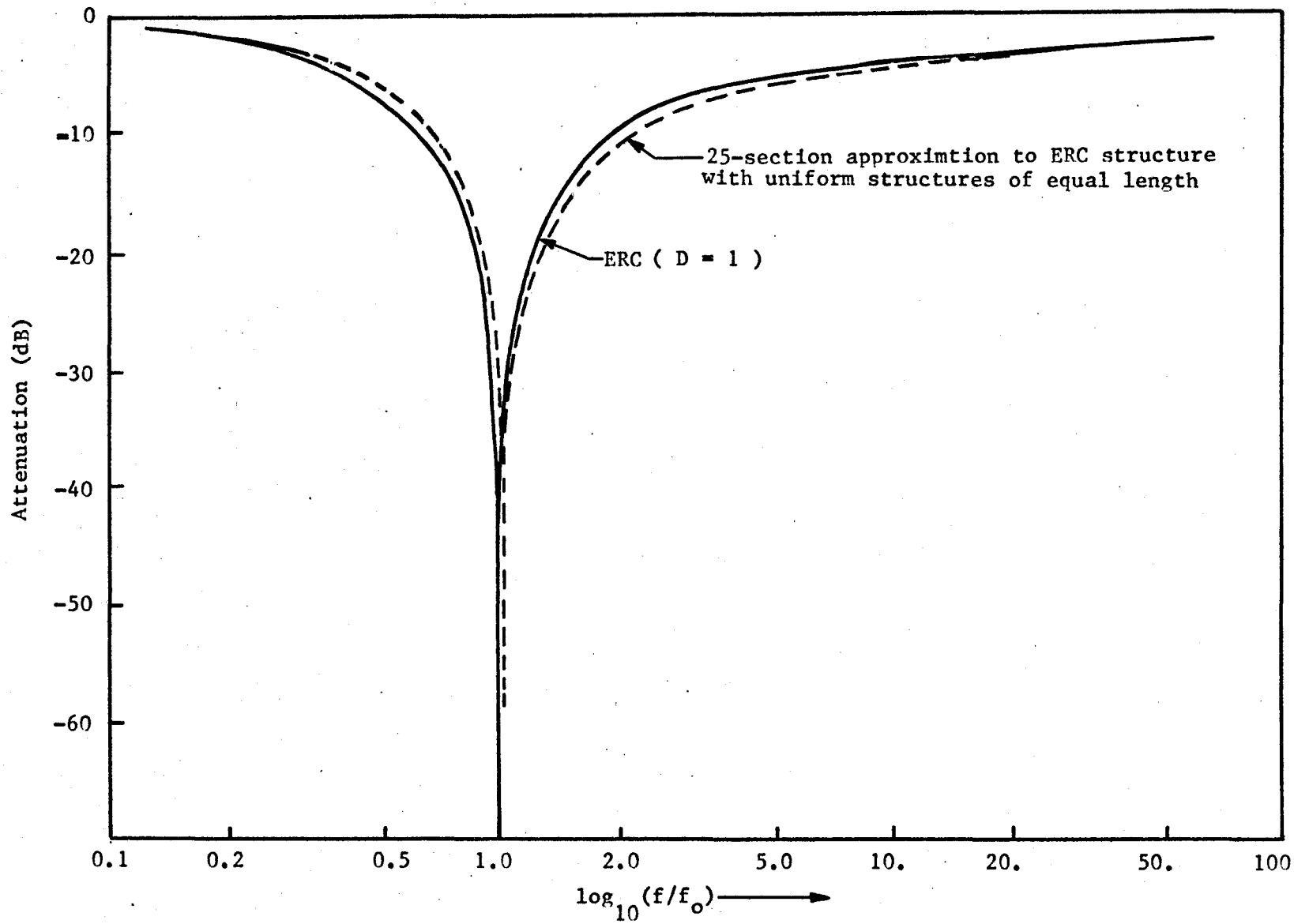

Figure 3.5

Comparison of notch response for (a)exponentially tapered (ERC) structure, (b) 25 section approximation

of equal length.

By procuring the ABCD parameters of the overall cascaded structure, where the ABCD parameters of each URC structure depend only on that structure's length and width,

$$\begin{bmatrix} A_T & B_T \\ C_T & D_T \end{bmatrix} = \sum_{n=1}^{k} \begin{bmatrix} A_n & B_n \\ C_n & D_n \end{bmatrix} \tag{3.8}$$

the open circuit transfer function may be obtained from a z parameter description of the network which is in turn acquired through manipulation of the ABCD parameters.

$$T_{O/C} = \frac{z_{21}}{z_{11}} = \frac{1}{A_T} \tag{3.9}$$

and the need for solving the differential equation (2.9), which will ultimately give the network transfer function, vanishes.

Now since it is the optimal electrical shape that must be obtained, then if the widths (for constant lengths) are varied, and the transfer function of these adjusted networks is obtained, some idea as to what constitutes an optimal shape may materialize.

But it is not only the shape of the structure that gives the match response, since the proper choice of the notch resistor R_N, also affects this response, as indicated in figure (2.9). Thus the optimization of the shape of the structure must be accompanied by optimization of the notch resistor at the same time !

3.4 Optimization Using Gradient Information

Once realizing the need for applying computer-aided design techniques to this network problem, further difficulties emerge since many useful computer-aided design methods of optimization are available.

As suggested by the subheading of this chapter, an "indirect" [21] method of computer-aided design, which uses the gradients of the objective function, is employed. This is chosen over other "indirect" methods because (a) it consumes less computer time, (b) it's relatively easy to calculate gradients for a many-sectioned network due to the cascaded nature of the problem, and (c) it was found to give better minimal performance measure and the resultant parameter gave a better notch response. Note that this is not usually the case, since both "indirect" and "direct" methods generally give the same result - but in this case noticeable disagreements arose !

From the gradient methods available that of Fletcher-Powell-Davidon [9] was chosen principally because of its established reliability, its general applicability, and its good documentation.

3.5 Appropriate Performance Measure

Even with a problem that is particularly suited to using computer-aided design techniques, together with one of the most reliable of these methods available, a "significant" improvement in design may not be attained if an ill-conceived performance measure is used. Ideally, the notch response desired is one of zero attenuation at all frequencies, save the notch frequency, which should have infinite attenuation.

The best formulation of the desired response (S), and hence,

objective function (U), was found to be as shown in figure 3.6.Where, in the region Δf, a maximum attenuation of -60 dB is specified at the single notch frequence, and is chosen as the upper specified response (S_u). An attenuation of 0 dB outside Δf is specified as the lower specified response (S_l).

If other frequency points (as well as notch frequency) in Δf are included as part of S_u, either at a constant -60 dB attenuation, or an attenuation which linearly decreases or increases from f_1 to f_o and f_o to f_2 respectively, then a least p^{th} objective formulation[1,2], will not yield a notch response.The tendency in the least p^{th} formulation is to reduce the maximum errors the most, and since in these will lie either side of f_o, for these cases the resultant optimized response will be more a band rejection than a notch response.

Thus, for the problem of finding the optimal thin-film shape, which will give the "best" notch response, the performance measure can be formulated in a least p^{th} sense, using the specifications of figure 3.6. With these notations, the performance measure for a "specifications violated" case, per Bandler and Charalambous[2] is

$$U = \sum_{i \in J_u} \left[e_{ui}(\underset{\sim}{\phi}) \right]^p + \sum_{i \in J_l} \left[-e_{li}(\underset{\sim}{\phi}) \right]^p \qquad (3.10)$$

where

$$J_u \triangleq \left\{ i \mid e_{ui}(\underset{\sim}{\phi}) \geq 0, i \in I_u \right\}$$

$$J_l \triangleq \left\{ i \mid -e_{li}(\underset{\sim}{\phi}) \geq 0, i \in I_l \right\}$$

$$e_{ui}(\underset{\sim}{\phi}) \triangleq e_u(\underset{\sim}{\phi}, \psi_i)$$

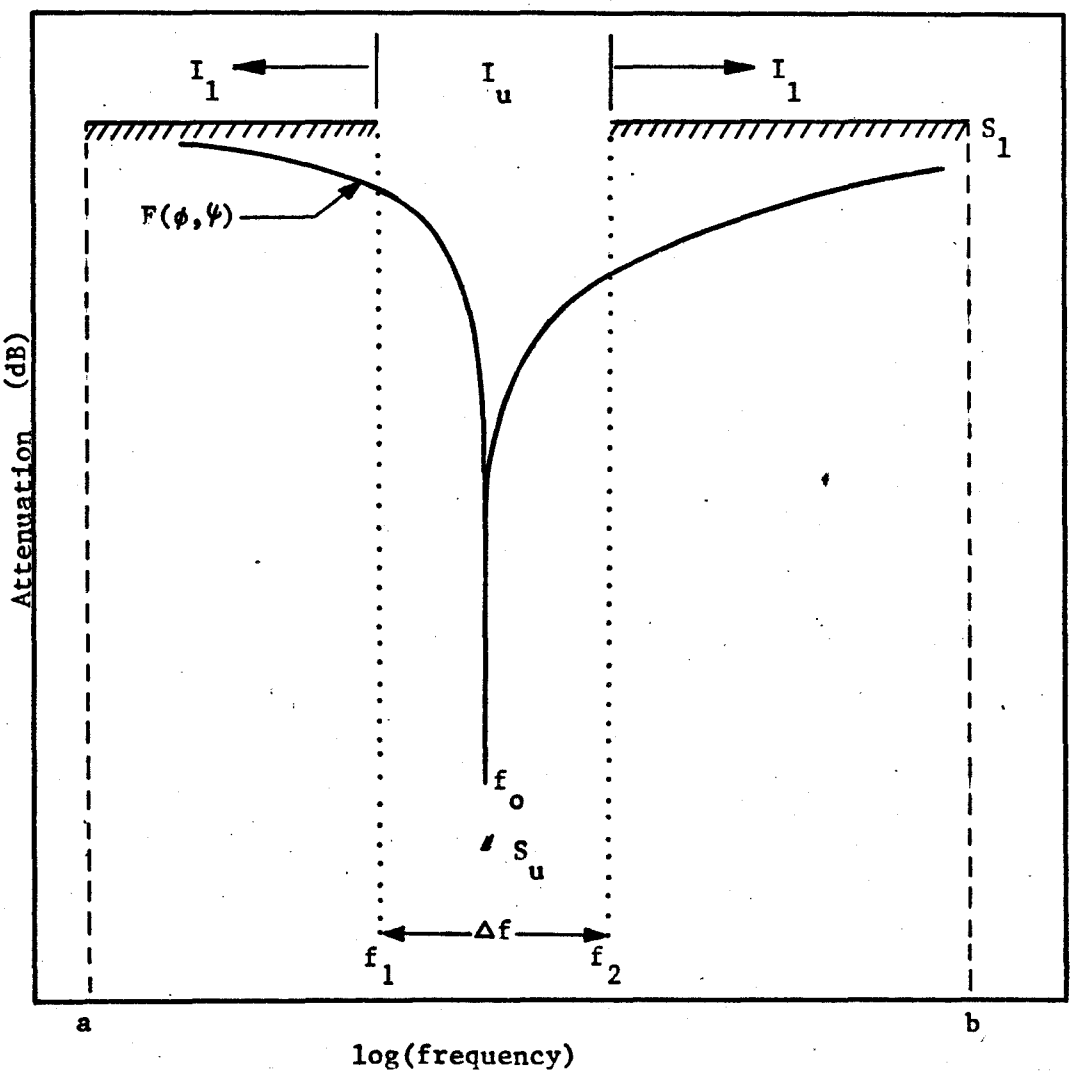

Figure 3.6

Pictoral representation of final formulation of objective function (U), and desired response (specified function - S).

$$e_{li}(\underset{\sim}{\phi}) \triangleq e_l(\underset{\sim}{\phi},\psi_i)$$

The considerations of "specifications violated" simply indicates that some, or all, of the $e_{ui}(\underset{\sim}{\phi})$ and $-e_{li}(\underset{\sim}{\phi})$ are positive, and the approximating function falls short of meeting,or improving upon, the specified function $S(\psi)$.

3.6 Practical Formulation of The Problem

3.6.1 General

The physical aspects of the problem must now be applied to the definitions and formulations previously discussed, so that a workable computer algorithm may be devised.

3.6.2 Gradient of Objective Function

If the optimization technique of Fletcher-Powell-Davidon is to be used, then the gradient of the objective function, (equation (3.10)) with respect to the design parameters, must be obtained. Thus

$$\underset{\sim}{\nabla}U = \left\{\sum_i\left[e_{ui}(\underset{\sim}{\phi})\right]^p + \sum_i\left[-e_{li}(\underset{\sim}{\phi})\right]^p\right\}^{\frac{1}{p}-1}\left\{\sum_i\left[e_{ui}(\underset{\sim}{\phi})\right]^{p-1}\underset{\sim}{\nabla}e_{ui}(\underset{\sim}{\phi}) - \sum_i\left[-e_{li}(\phi)\right]^{p-1}\underset{\sim}{\nabla}e_{li}(\underset{\sim}{\phi})\right\} \tag{3.11}$$

where now the norm[1] of the objective function is considered in the algorithm. Now, assuming $\omega = 1$, the task is to find

$$\underset{\sim}{\nabla}e(\underset{\sim}{\phi}) = \underset{\sim}{\nabla}\left[F(\underset{\sim}{\phi},\psi) - S(\psi)\right] \tag{3.12}$$

$$= \underset{\sim}{\nabla}F(\underset{\sim}{\phi},\psi) \tag{3.13}$$

since

$$\frac{\partial S(\psi)}{\partial \underset{\sim}{\phi}} = 0$$

In this problem $F(\underset{\sim}{\phi},\psi)$ was the open circuit voltage transfer function of a URC notch filter. Hence

$$F(\underset{\sim}{\phi},\psi) = 20 \log_{10}\left|\frac{V_{out}}{V_{in}}\right| \tag{3.14}$$

where in this case V_{out} and V_{in} are complex functions of frequency. If V_{out}/V_{in} is represented by T, and the partial derivatives of $F(\underset{\sim}{\phi},\psi)$ are taken with respect to the circuit adjustable parameters $\underset{\sim}{\phi}$, then

$$\frac{\partial F(\underset{\sim}{\phi},\psi)}{\partial \underset{\sim}{\phi}} = 20\frac{\log_{10} e}{|T|^2}\,\mathrm{Re}(T^* \underset{\sim}{\nabla} T) \tag{3.15}$$

The problem now concerns the question of determining $\underset{\sim}{\nabla} T$. For if T $(= V_{out}/V_{in})$ is obtained by cascading many URC structures, then, as indicated in reference 2, there is great difficulty in determining the gradient of T with respect to some middle-section parameter.

But fortunately there has recently been developed a network algorithm [7], which gives the necessary gradient information after performing only two complete network analyses, regardless of the number of parameters involved.This involves the use of the original network and its adjoint [7].Only the essential ideas of this paper and a subsequent one by Bandler and Seviora [3] will be presented here.

If the notation of figure 3.7 is used, then

$$T = \frac{V_{out}}{Vin} \tag{3.16}$$

and

$$\underset{\sim}{\nabla} T = \frac{V_{in}\,\underset{\sim}{\nabla} V_{out} - V_{out}\,\underset{\sim}{\nabla} V_{in}}{V_{in}^{\,2}}$$

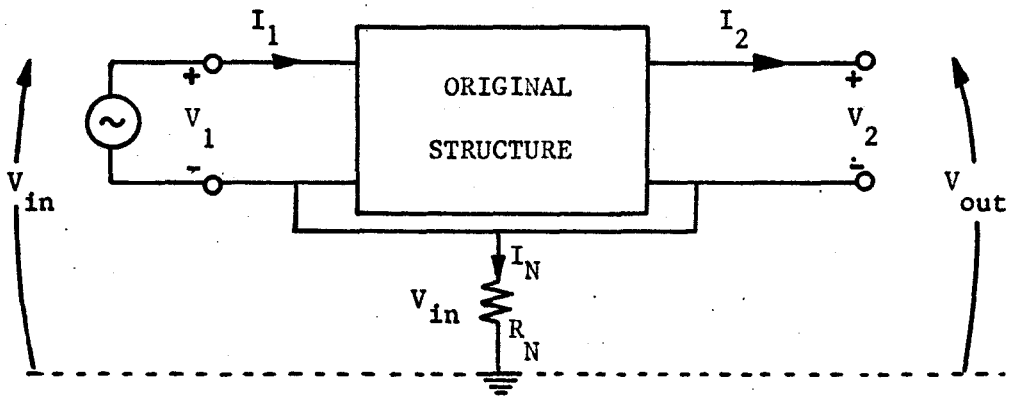

Since V_{out} is open circuited, $I_2=0$, hence V_2 may be set to 1 volt. Then

$$\begin{aligned} V_{in} &= V_N + V_1 \\ &= I_N R_N + V_1 \\ &= I_1 R_N + V_1 \end{aligned}$$

Figure 3.7

Original cascaded URC structure (with notch resistor) showing voltage and current conditions at its ports.

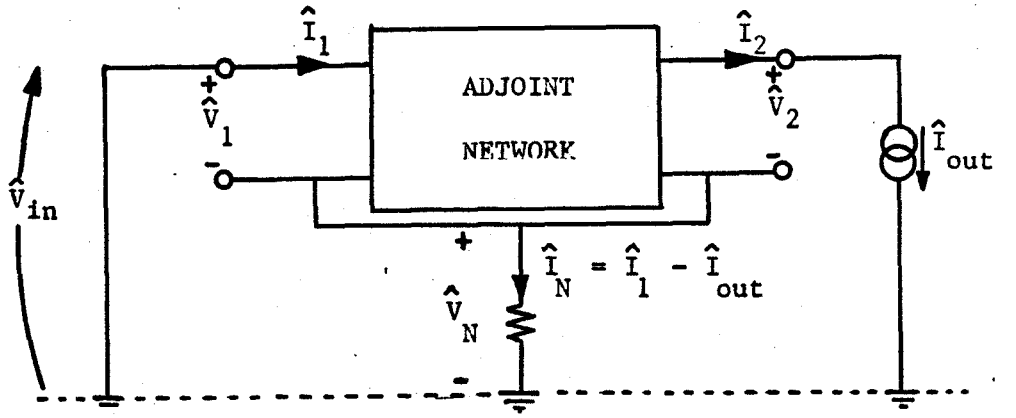

Since $\hat{V}_{in}$ is short circuited, $\hat{V}_{in}=0$, hence $\hat{I}_1$ may be set to 1 amp. Then it may be shown that

$$\hat{V}_1 = -(\hat{I}_1 - \hat{I}_{out})R_N$$

Figure 3.8

Adjoint network of cascaded URC structure (with notch resistor) showing voltage and current conditions at its ports.

$$= \frac{1}{V_{in}} \underset{\sim}{\nabla} V_{out} \tag{3.17}$$

By invoking what is termed the "useful equation" of reference 3, it can be demonstrated that the excitations of the original and adjoint networks are as shown in figure 3.7 and 3.8 respectively. Also that

$$\underset{\sim}{\nabla} T = \frac{1}{V_{in}} \frac{1}{\hat{I}_{out}} \underset{\sim}{G} \tag{3.18}$$

where, $\hat{}$ denotes the responses or excitations of the adjoint network

$\underset{\sim}{G}$ is a vector of sensitivities related to the adjustable network parameters contained in $\underset{\sim}{\phi}$.

The form of $\underset{\sim}{G}$ may be obtained from Table II of reference 3 for a uniformly distributed RC transmission line. And since Z_o can be shown to be only a function of W (the section width) then

$$\frac{dZ_{o_i}}{dW_i} = -\frac{1}{W_i} Z_{o_i} \tag{3.19}$$

By combining the results of equations (3.15), (3.18), and (3.19) with the appropriate sensitivity $\underset{\sim}{G}$, the relevant gradient of the network transfer function, with respect to the parameters to be adjusted, will be found to be

$$\frac{\partial F(W_i, \Psi)}{\partial W_i} = 20 \frac{\log_{10} e}{|T|^2} \operatorname{Re} \left\{ T^* \left[\frac{1}{W_i} \left[V_i \hat{I}_i - V_{i+1} \hat{I}_{i+1} \right] \right] \right\} \tag{3.20}$$

where the adjustable parameters $\underset{\sim}{\phi}$, are now the widths W_i, of the URC sections.

3.7 Parameter Constraints

Because of substrate size, and minimally deposited width limitations, the widths of the structures must have constraints, where the lower bound (ϕ_1) is 0.005 cm., and the upper bound (ϕ_u) is 1.9 cm. (for a 2 cm. by 2 cm. substrate). The function which will give widths that will be constrained to vary within these bounds is

$$\phi_i = \phi_{1i} + (\phi_{ui} - \phi_{1i}) \sin^2(\phi_i') \tag{3.21}$$

Also since R_N is another parameter to be optimized, and it can never have real negative values, the constraint used to ensure positive notch resistances, was

$$\phi_i = \exp(\phi_i') \tag{3.22}$$

Where in equations (3.21) and (3.22) ϕ_i' instead of ϕ_i become the circuit adjustable parameters. Note that the gradients must be changed accordingly, as shown in equation (3.23).

$$\frac{\partial F(\phi_i, \psi)}{\partial \phi_i'} = \frac{\partial F(\phi_i, \psi)}{\partial \phi_i} \frac{\partial \phi_i}{\partial \phi_i'} \tag{3.23}$$

3.8 Weighting Factors

Since only one point inside Δf (figure 3.6) is used in the objective function, it may be expected that more weight be added to this error, to make it "compatible" with the sum of the errors outside Δf. But a weight of 1 was used since any value greater than 1 placed too much emphasis on the notch frequency.

CHAPTER 4

COMPUTER-AIDED DESIGN RESULTS

4.1 The Data Obtained

The design algorithm was programmed on the CDC-6400 Digital Computer facility at McMaster University, using Fortran IV programming language. The algorithm of Fletcher-Powell-Davidon was also implemented on the CDC 6400, where it is contained as a computer-library subroutine. Its program listing may be obtained from McMaster's computer department.

Due to, (a) the discontinuous nature of the response that is sought, (b) the notch response of a URC notch network is readily obtainable, and (c) the effects of computer-aided design techniques on the problem are not predictable; it was decided to begin the design by cascading just two uniform RC structures.

The results of this Fletcher-Powell-Davidon optimization, which include the starting widths, notch resistance, corresponding objective function, and resultant attenuations, are given in column two of Table 4.1. A reasonable conclusion would be that these optimized parameters sought the limits of the extremes imposed on the parameters - namely 1.9 cm. and 0.005 cm. This may not be so pertinent a discovery, were it not for the results that accrue when a 3,4,5 and 6 section network is optimized.

The results of the optimization of the widths and notch resistance, of the 3,4,5 and 6 section networks, appear in column two

Table 4.1

Starting and optimized parameters, objective function, and gain, for the 2-section network.

	Start	Fletcher-Powell-Davidon optimization	Nominal grid search optimization
Gain(dB)	-39.4	-37.8	-66.7
U	22.24	17.1	17.05
W_1 (cm)	1.0	1.868	1.868
W_2 (cm)	1.0	0.005	0.005
R_N (Ω)	3.12	3.208	2.998

Table 4.2

Starting and optimized parameters, objective function, and gain, for the 3-section network.

	Start	Fletcher-Powell-Davidon optimization	Nominal grid search optimization
Gain(dB)	-24.0	-47.6	-73.4
U	32.36	5.7	5.7
W_1 (cm)	1.7	1.868	1.868
W_2 (cm)	.00500001	0.0776	0.0776
W_3 (cm)	.00500001	0.005	0.005
R_N (Ω)	.177	4.237	4.27

Table 4.3

Starting and optimized parameters, objective function, and gain, for the 4-section network.

	Start	Fletcher-Powell-Davidon optimization	Nominal grid search optimization
Gain(dB)	-22.8	-38.8	-79.8
U	33.1	27.3	16.06
W_1 (cm)	1.7	1.9	1.9
W_2 (cm)	..017	.269	.269
W_3 (cm)	.00500001	.037	.037
W_4 (cm)	.00500001	.005	.005
R_N (Ω)	.190	4.295	4.798

Table 4.4

Starting and optimized parameters, objective function, and gain, for the 5-section network.

	Start	Fletcher-Powell-Davidon optimization	Nominal grid search optimization
Gain(dB)	-22.4	-39.3	-58.3
U	32.9	27.1	17.2
W_1 (cm)	1.7	1.9	1.9
W_2 (cm)	.12	.219	.219
W_3 (cm)	.017	.069	.069
W_4 (cm)	.006	.015	.015
W_5 (cm)	.00500001	.005	.005
R_N (Ω)	.190	5.716	5.9

Table 4.5

Starting and optimized parameters, objective function, and gain, for the 6-section network.

	Start	Fletcher-Powell-Davidon optimization	Nominal grid search optimization
Gain(dB)	-22.2	-43.3	-68.9
U	35.9	23.6	12.1
W_1 (cm)	1.7	1.9	1.9
W_2 (cm)	.12	.48	.48
W_3 (cm)	.12	.159	.159
W_4 (cm)	.007	.050	.050
W_5 (cm)	.00500001	.015	.015
W_6 (cm)	.00500001	.005	.005
R_N (Ω)	.190	5.51	5.753

of Tables 4.2 to 4.5, respectively. In all instances, these widths "fill in the gaps" between the extreme limits that are imposed on these parameters. They do so in some well-defined fashion, which is brought to light in figures 4.1 to 4.4. The evidence here indicates that the widths define a shape that is exponentially tapered. And if the same notation is used as in the reference of Carson [5], the "degree of taper" (D) is between 3.5 and 4.5.

But before this evidence is examined, a slight digression should be made to explain the entries in column three of Tables 4.1 to 4.5. In the method of Fletcher-Powell-Davidon, the capacitance per unit square, resistance per unit square, and length were held constant, while the widths of each section were allowed to vary. When the optimal widths are located, the total resistance (R) and capacitance (C) of the network becomes fixed, and an optimal notch is obtained. When this is coupled with the calculation of the transfer function in the region about the notch, at discrete 4 KHz intervals, resultant attenuations for the designed networks do not meet the requirements of a -60 dB notch.

This may be explained through the realization, that the position of the notch is governed by the RC product of the structure. Any slight variation of either R or C will disturb the notch off its optimal value. Since the optimal notch resistance of the network has been located by Fletcher-Powell-Davidon minimization technique, this necessarily must freeze the total resistance at its starting value. Thus the only avenue to explore, and thereby obtain better attenuations, is the variation of the structure capacitance (C).

A nominal grid search (positive or negative incremental additions) of the structure capacitance was then performed. The aim was not to obtain the optimal structure capacitance, but to improve the attenuations of the notch network which were largely affected by discrete frequency calculations. Along with these changes, slight grid search modifications of the notch resistor were also prescribed. Column three of Tables 4.1 to 4.5, indicates the improvements rendered when these minimal modifications were adopted.

4.2 The Resultant Shape Obtained

From the curves of figures 4.1 to 4.4, the circled points that appear on these graphs, are the points corresponding to the optimized widths, at mid-lengths, of the cascaded network. The smooth curve formed through (or almost through) these points, represents an exponential least squares fit of the (x,y) coordinates of the points on each graph. The regression fit was performed on a Hewlett-Packard 9100A Desk Calculator, and 9125A Calculator Plotter.

The resultant curve that forms, $y = e \exp(bx)$, is shown in the actual plot. And, if $\lambda = 1$ cm., and $D = m\lambda/2$ (where m is the power of the exponential function), the values of 3.54 to 4.45 can be obtained for D.

Also from the least squares method, the "correlation coefficient" (r) is obtained. If the exponential form of the curve is $y = a\, e^{mx}$, this can be linearized to

$$\ln(y) = \ln(a) + mx \qquad (4.1)$$

or

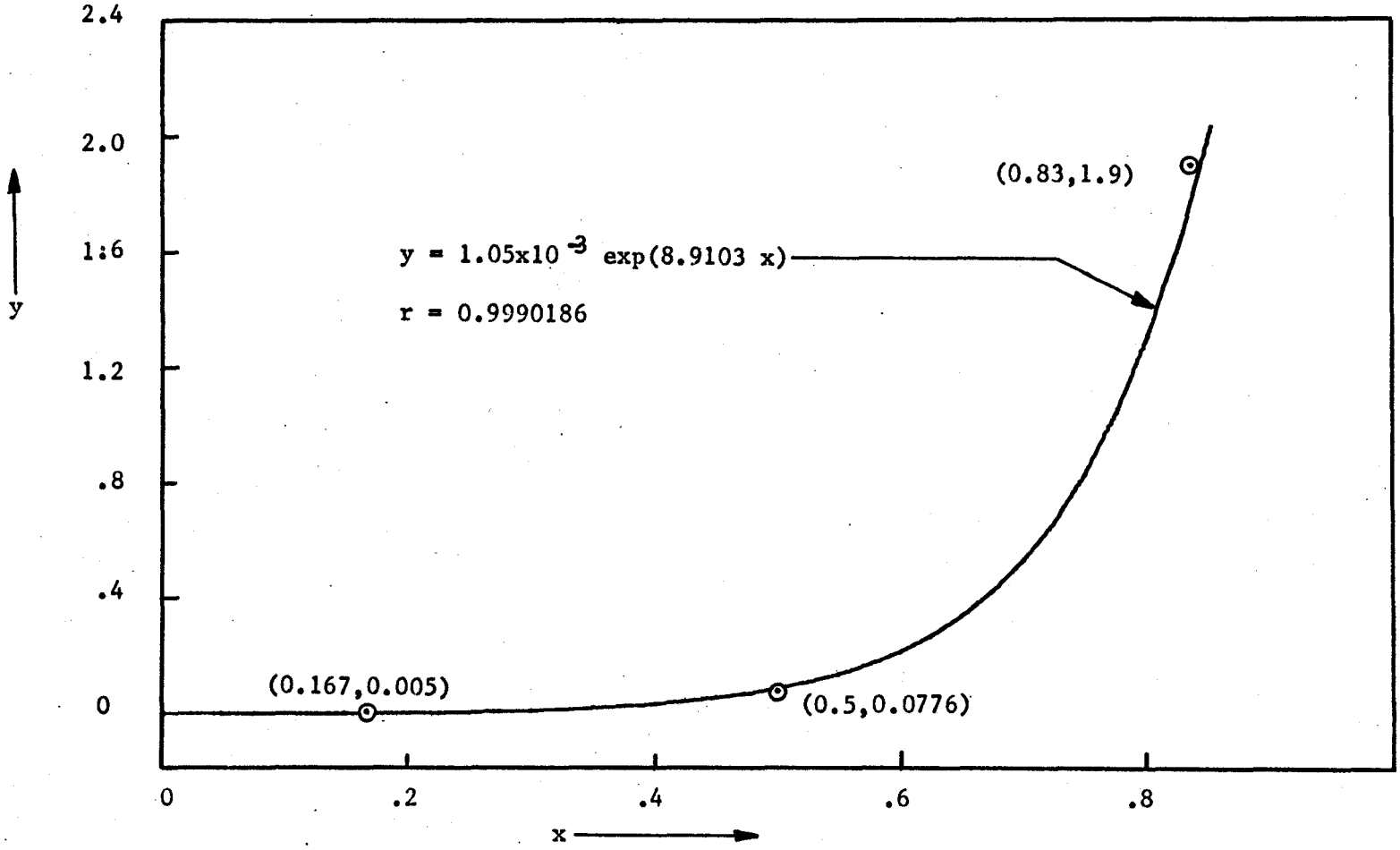

Figure 4.1

Exponential least squares regression fit of optimized widths of 3-section cascaded network.

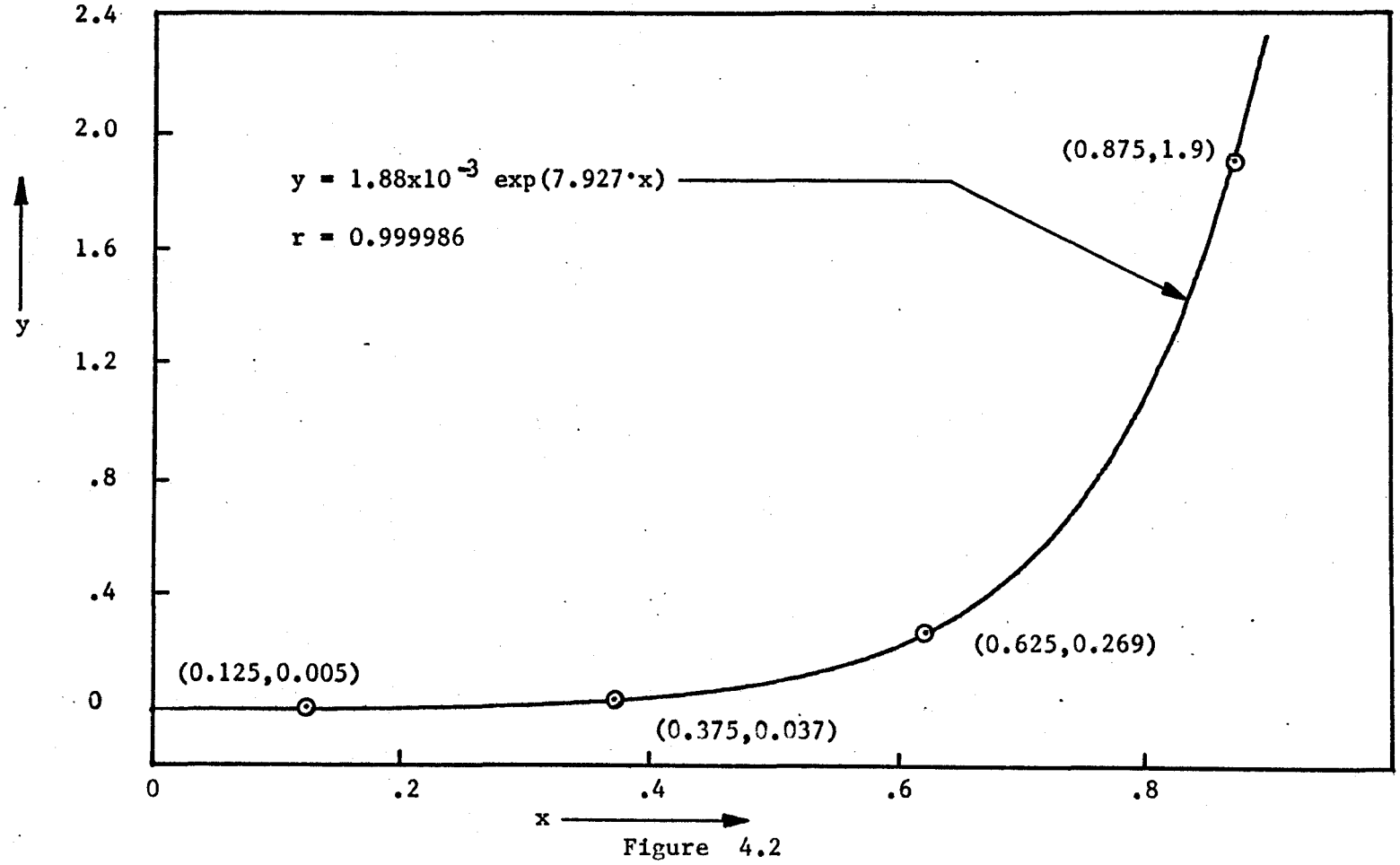

Figure 4.2

Exponential least squares regression fit of optimized widths of 4-section cascaded network.

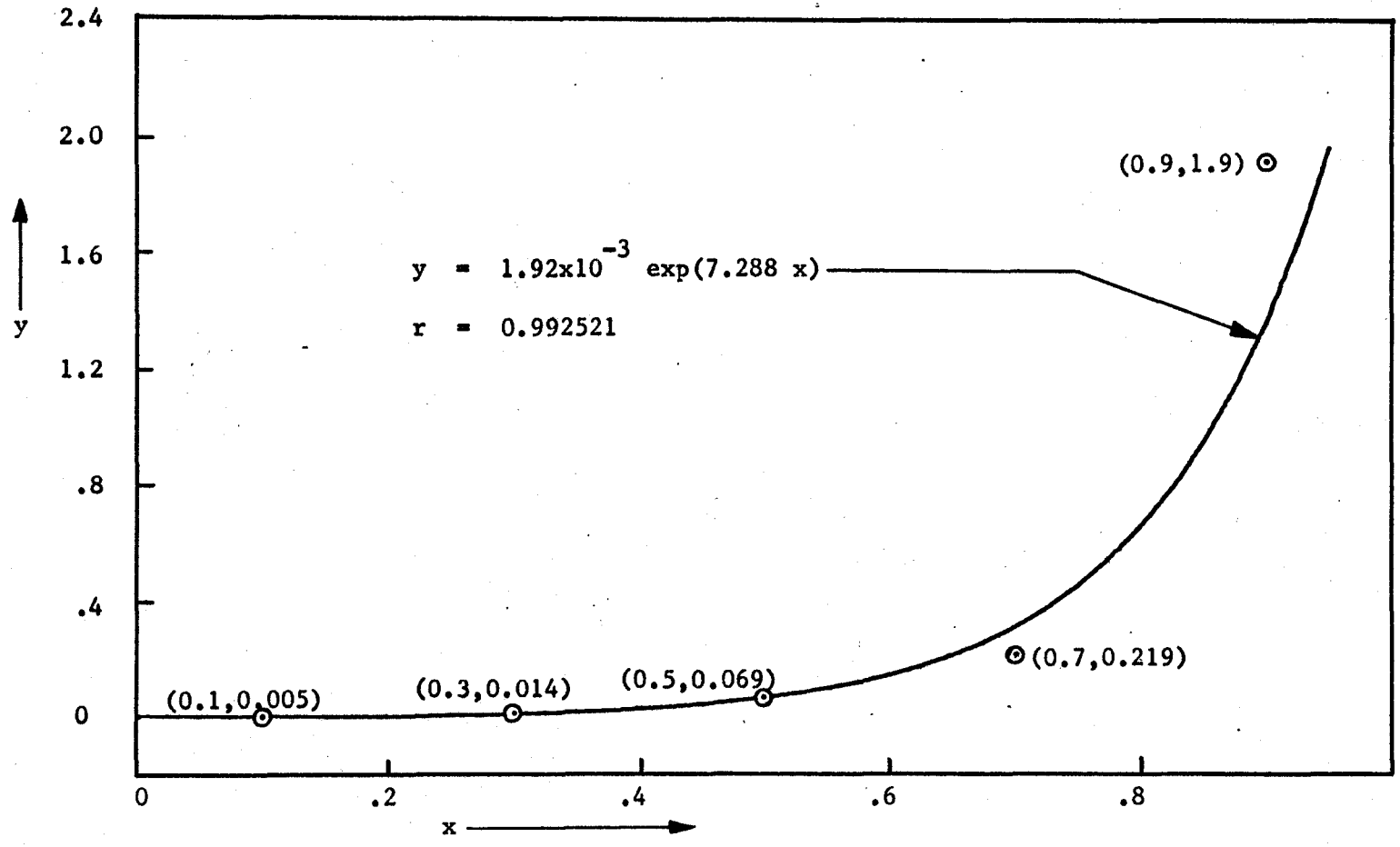

Figure 4.3

Exponential least squares regression fit of optimized widths of 5-section cascaded network.

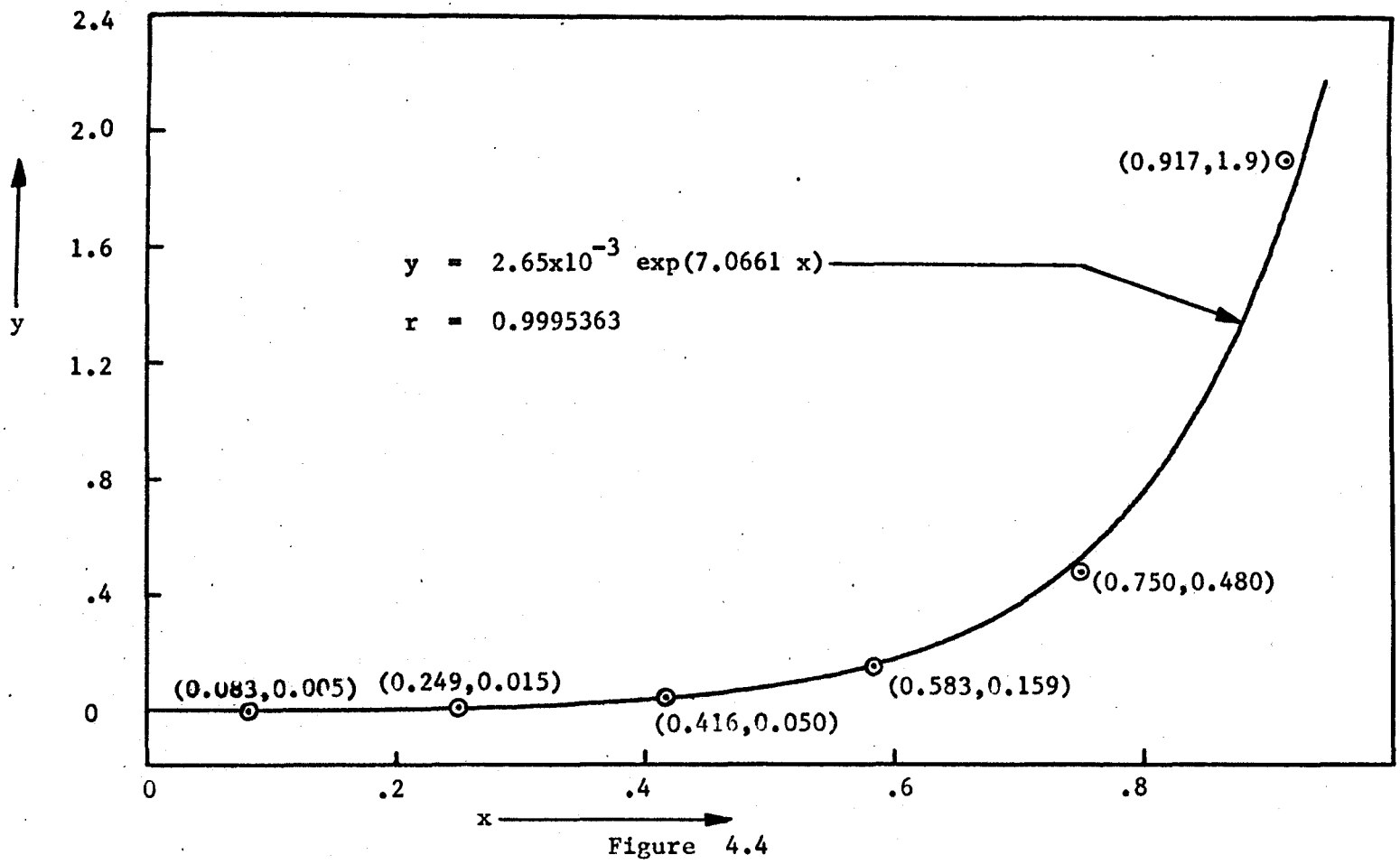

Figure 4.4

Exponential least squares regression fit of optimized widths of 6-section cascaded network.

$$Y = A + mx \tag{4.2}$$

Then the correlation coefficient is given by

$$r = \frac{n\sum xY - \sum x\sum Y}{\sqrt{(n\sum x^2 - (\sum x)^2)(n\sum Y^2 - (\sum Y)^2)}} \tag{4.3}$$

where n is the number of data points to be "fitted", The closer r is to 1.0 , then the better the exponential curve "fits" the data. A survey of the r's obtained, also strengthens the argument that these widths are exponentially increasing , particularly in the cases of the 4 and 6 section structures.

An additional observation, may be the fact that the power of the exponential (m), appears to be decreasing and converging (8.9,7.9, 7.3,7.1) as the number of sections increases from 2 to 6. Rather strong evidence points to the conclusion that a value of about 7.0, for an infinite number of cascaded sections, would be the power of a continuous exponentially tapered structure. Thus the "degree of taper" would be 3.5 for a 1 centimetre long structure.

4.3 Comparison of Theorectical Open Circuit Voltage Transfer Functions

Few comments may be made, since the improvements of the optimized shapes over other previously constructed circuits, when comparing notch responses, are readily apparent from figures 4.5, 4.6 and 4.7. These figures compare attenuations on a $\log_{10}$ normalized frequency, with the notch frequency (f_o) the normalizing factor.

As observed by Carson[5] , and repeated for the sake of comparison

an ERC notch network of D = 1.0, shows markedly improved bandwidth rejection response, when contrasted with the response of a URC notch network. But of greater significance in figure 4.5, is the theoretical response curve from Walsh and Close[27], obtained through computer-aided design of a thin-film RC structure, and the response curve of an optimal 2-section cascaded structure, obtained by the computer-aided design method described in this thesis.

The former, exhibits good symmetry about the notch frequency, but poor bandwidth rejection response. The latter is not as symmetrical but shows still better bandwidth rejection response than the REC notch network. Figure 4.6 then contrasts response curves of all subsequent design shapes, that result from using the design algorithm proposed herein. Note that the 6-section optimal design, shows only very slight improvements in response, over the 4-section design. But the improvements of the 4-section response curve, are much larger when compared to those of the 2-section response curve. Figure 4.7 gives a final look at the theoretical notch response of a structure that was previously fabricated (the ERC) and the optimally designed 6-section network, as determined in this thesis.

Conspicuous by virtue of their absence, are the notch response curves for the optimally determined structures of 3 and 5 cascaded sections. These were omitted because they simply fill in the spaces between the response curves of the 2- and 4-section design, and the 4- and 6-section design. No additional information may be obtained if these were added.

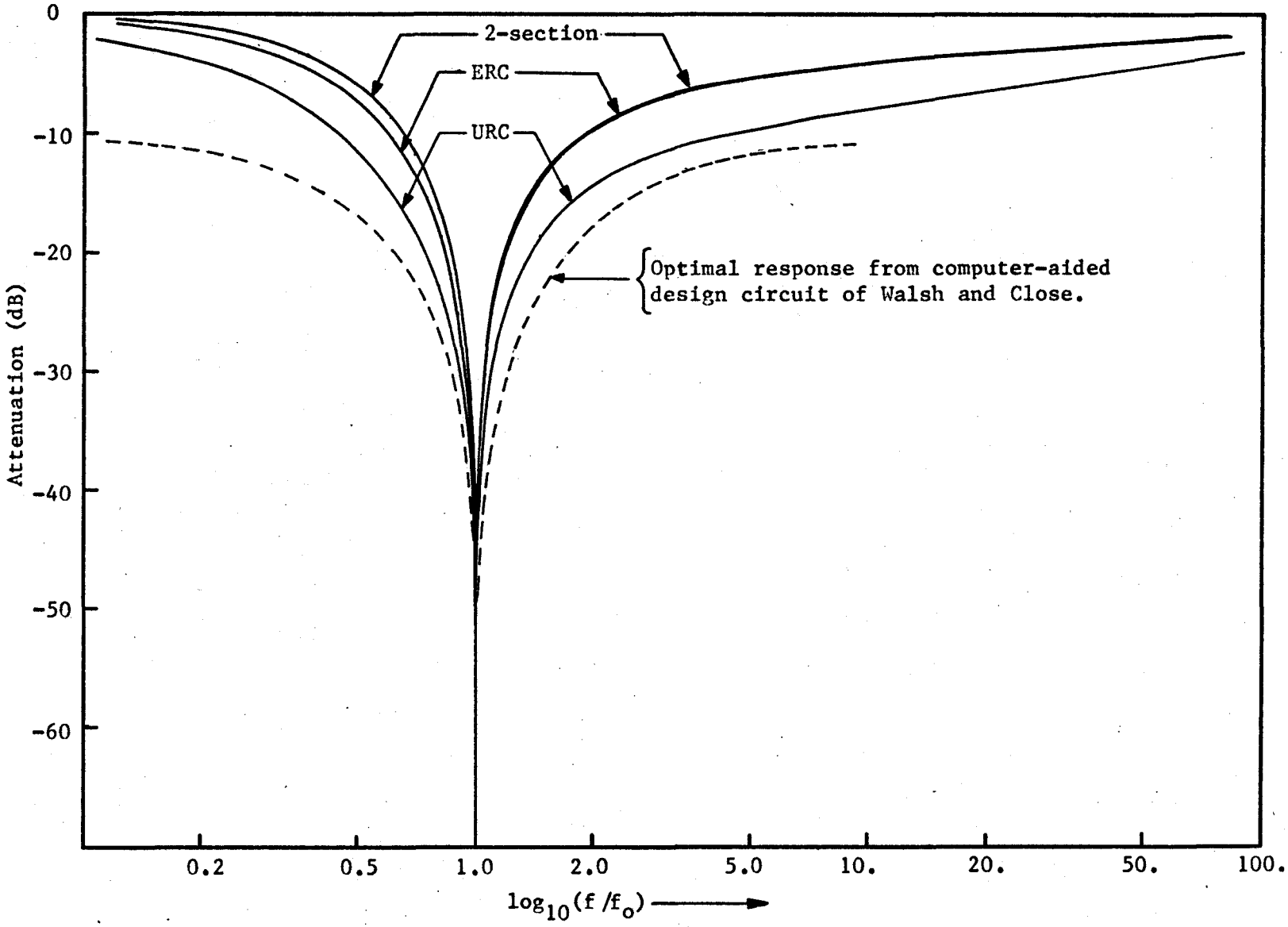

Figure 4.5

Comparison of some earlier notch network responses, with optimal 2-section notch response.

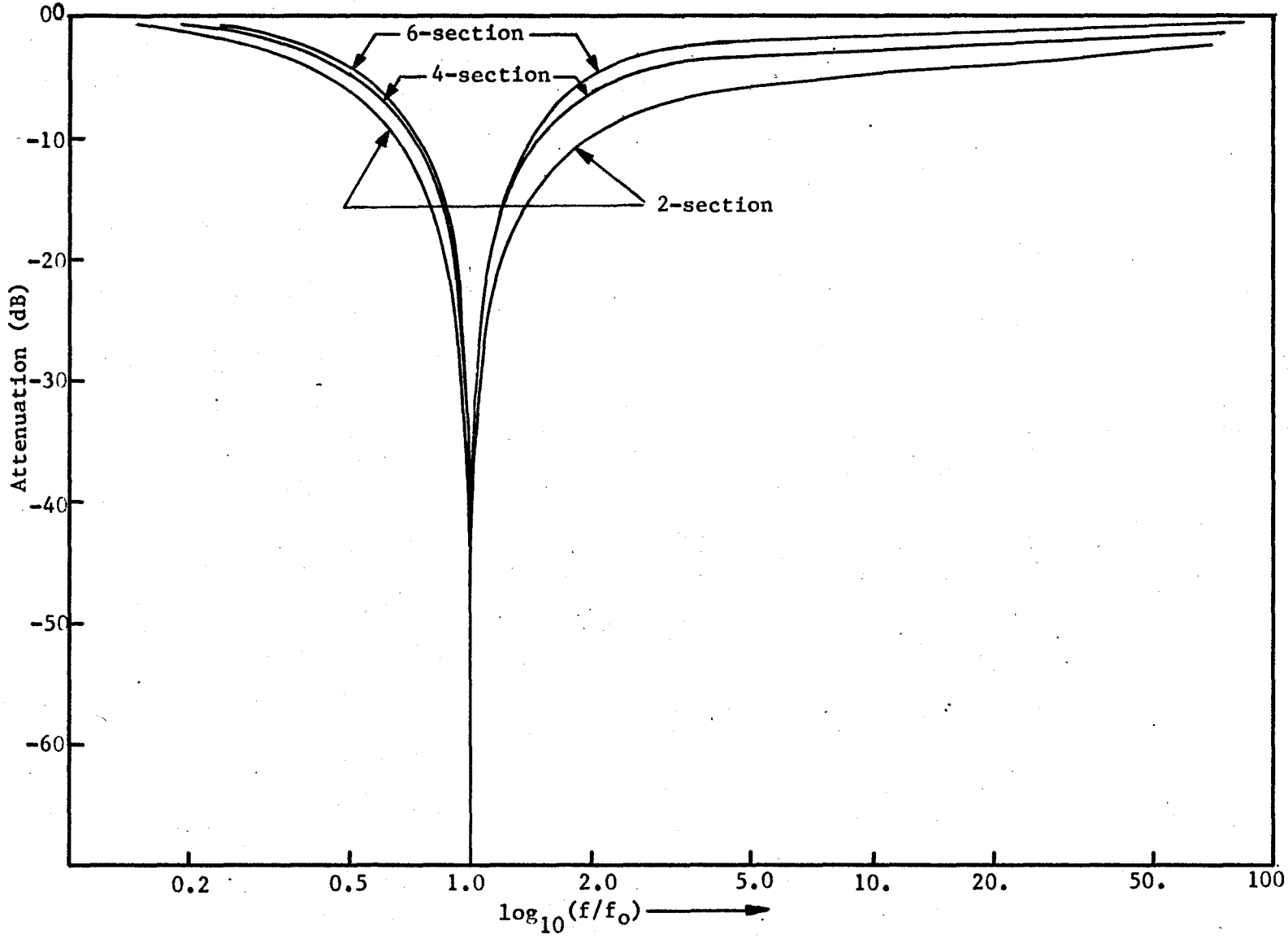

Figure 4.6

Comparison of optimal 2-, 4- and 6-section notch network responses.

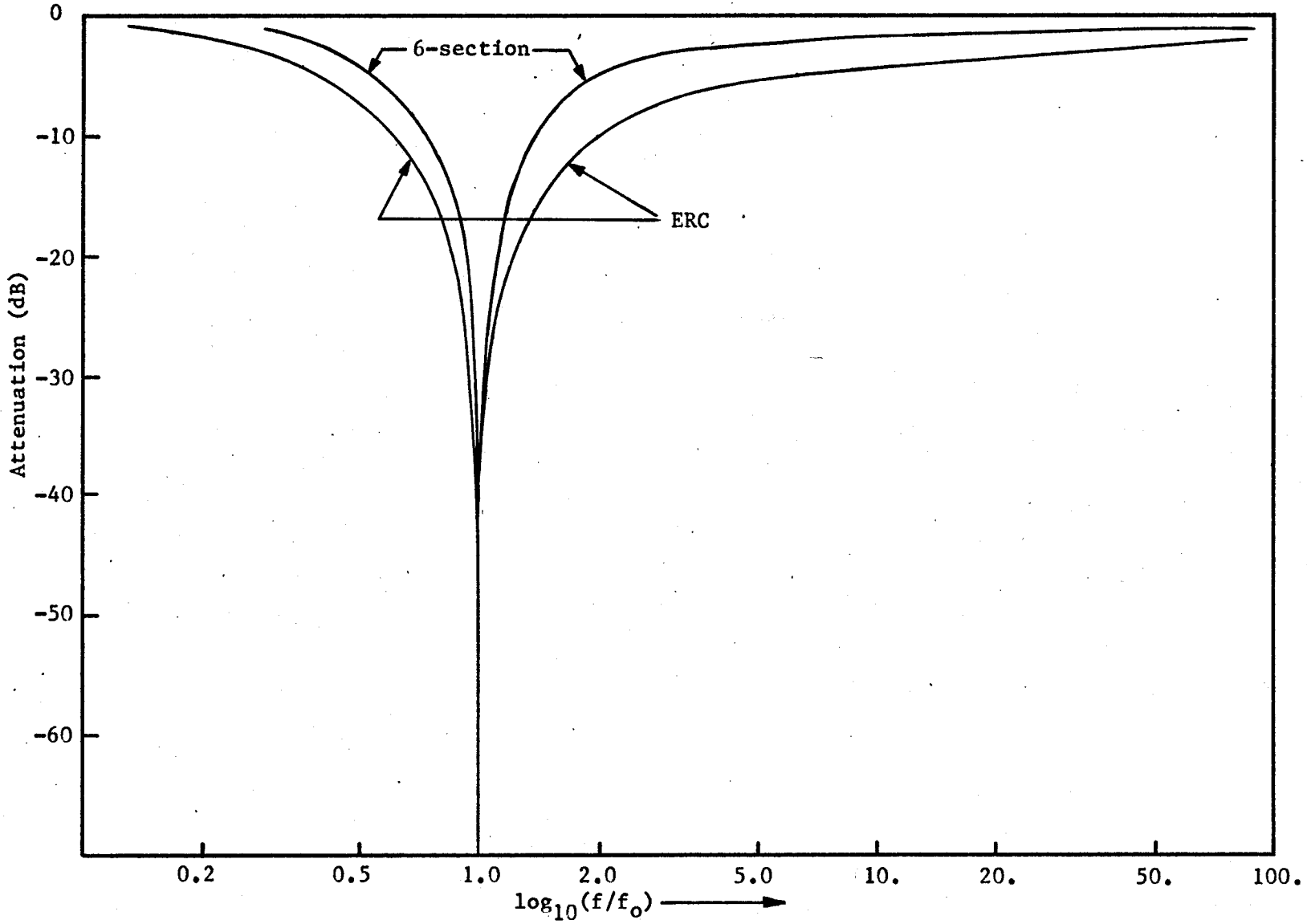

Figure 4.7

Comparison of ERC (D = +1), and optimal 6-section, notch responses.

CHAPTER 5

FABRICATION OF THIN-FILM STRUCTURES, AND EXPERIMENTAL RESULTS

5.1 Thin-Film Distributed Circuits

A thin-film RC structure, as depicted in figure 2.3, may be constructed of materials such as Nichrome (for the resistive later), Yttrium Oxide (for the insulating layer), and Aluminum (for the highly conducting ground plane). These materials may be deposited on a silica or glass substrate, in an evapourated vacuum chamber. But the yield rate from this method is sometimes not heartening, and a large quantity of devices may need to be fabricated, before satisfactory results can be obtained. Also, at times they are quite "unstable", one day exhibiting predictable characteristics, and the next day behaving erratically. This may probably be due to poor handling of specimens, and/or improper care in storage.

Also because of device dimensions, and the high frequencies of operation, even slight parasitic inductances may adversely affect the response, particularly if the exist in the notch resistance leg [26]. For these reasons, and others that will evolve as the discussion progresses, it was considered more adaptable to construct the thin-film circuits with large-scale models of Mylar and Teledeltos.

5.2 Mylar-Teledeltos Models

5.2.1 General

The Teledeltos sheet is a 0.002 inch thick homogeneous, partially conducting material, with a nominal ρ of 2.0 ohms per square, which was used as the resistive layer of the thin-film network models. The Mylar sheet, - polyester film called ployethylene terephthalates (0.003 inches thick), was used as the insulating layer. It has a relative permittivity of 2.98, and a dissipation factor of 0.016, at 1 MHz. For the conducting plane, sheets of copper foil (0.002 and 0.003 inches thick) were deemed suitable.

The most attractive feature of adopting the use of these models is that the shape of the structure may be effortlessly altered by removing unnecessary parts with a knife, or scissors. Even reconstructing a structure, involves nothing more than cutting the appropriate shape out of the Teledeltos sheet and copper foil.

Contrast this with thin-film circuits, where large scale drawings (20X) of the structure must be photographed, and the appropriate masks (usually four) be etched. Then the evapouration of one layer per evacuation, in the vacuum unit, be performed. An unwarranted time-consumming process, if only small changes in the circuit configuration are desired.

But these Mylar-Teledeltos models also have limitations, as will become apparent in further discussions.

5.2.2 The Structures

The following model shapes were constructed; (a) URC (4 inches square),(b) ERC (D = 1), (c) 4-section optimal design, (d) 6-section.

By virtue of the conclusions previously formed in section 4.1 of this thesis; the optimized widths, when fitted with a smooth curve, display the form of an exponentially tapered structure.Thus the problem of how to fabricate these structures, to show optimal design improvements over other structures, must be solved. For the circuits which are exponentially tapered, it becomes necessary to transform the exponential electrical taper to a geometrical taper, so that equipotential boundaries are maintained. A curvilinear square approximation must be executed upon these exponential electrical tapers If this is done, a comparison of the original (electrical) and geometrical (curvilinear square approximation) shape is shown in figures 5.1 and 5.2.

As the taper becomes larger (D increases), the circuits that must be constructed (geometrical shape) become less attractive from a fabrication point of view. The aspect ratio becomes increasingly larger, as the "degree of taper" increases. For an exponential taper of D = 3.5, it would be an insurmountable task to fabricate it, and obtain the prescribed current flow. Consequently, the cascaded URC sections, with the optimially determined widths, were fabricated.

But even in this case, problems with maintaining uniform current flow and consistent equipotential boundaries must be overcome. If the sections are simply interconnected by joining them, as in figure 5.3, the lines of constant flux are greatly distorted , and values of resistance per unit length (r_o) and capacitance per unit length (c_o) are meaningless To retain these values, strips of conducting material must be placed between cascaded segments, as shown in figure 5.4. This maintains parallel lines of constant flux, and equipotential boundaries. A pictorial repre-

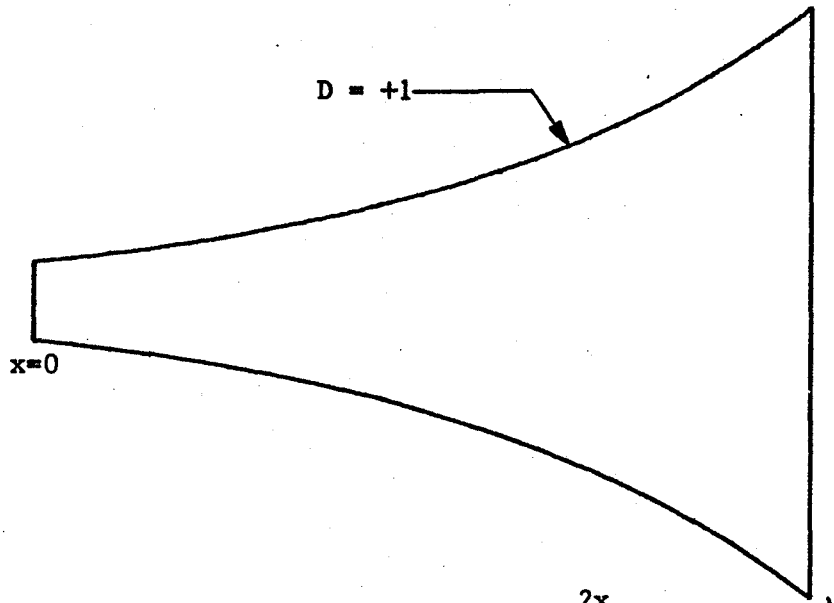

(a) Electrical taper $y = 0.05\, e^{2x}$

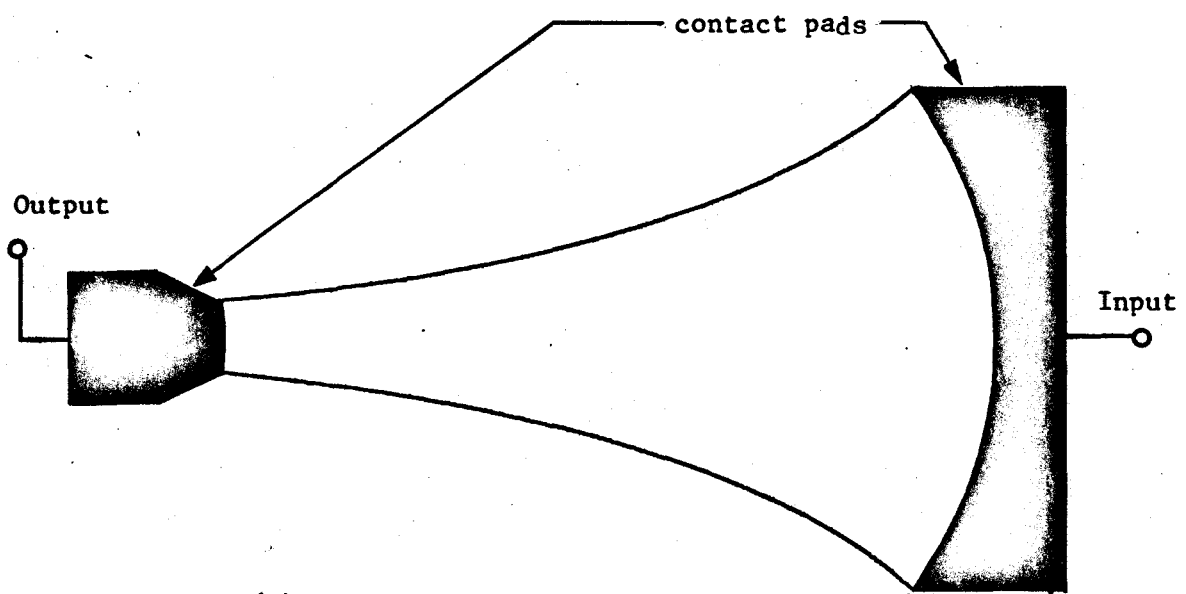

(b) Curvilinear square approximarion of (a)

Figure 5.1

Comparison in actual size of (a) electrical taper (D = 1), and (b) geometrical taper - curvilinear square approximation of (a)

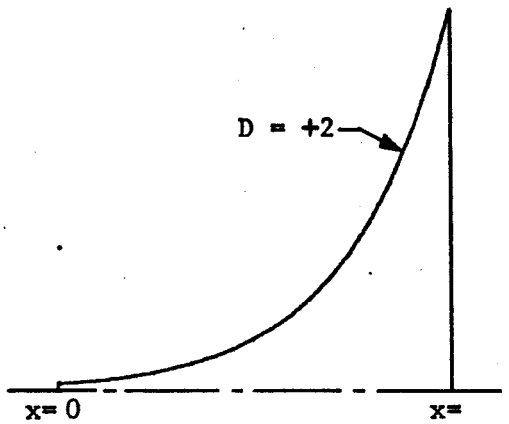

(a) Half-scale outline of electrical taper $y = 0.0175e^{4x}$

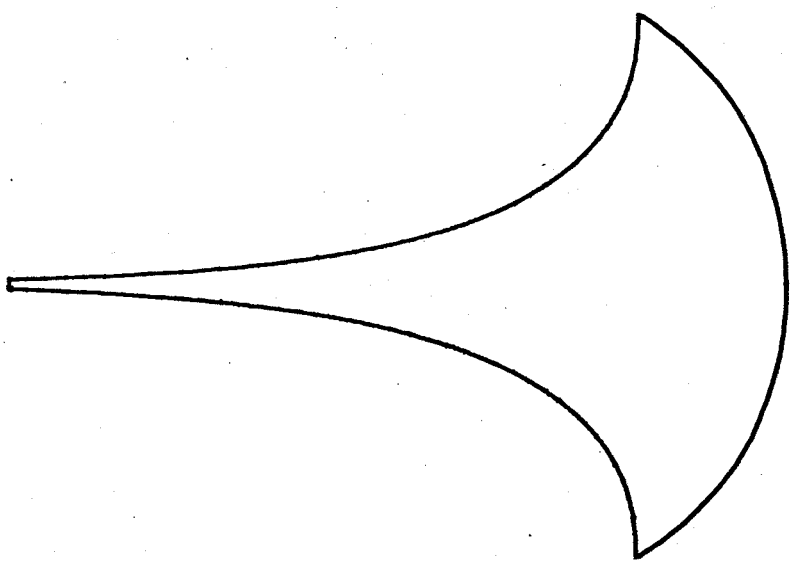

(b) Curvilinear square approximation of (a)

Figure 5.2

Comparison of (a) half-scale size of electrical taper (D = + 2) and (b) actual size of curvilinear square approximation to (a)

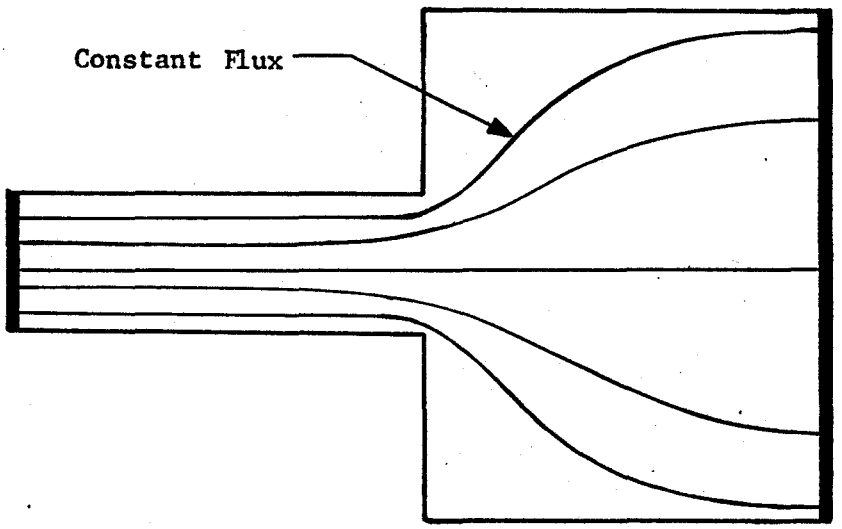

Figure 5.3

Current flow in a cascaded structure, without a conducting strip.

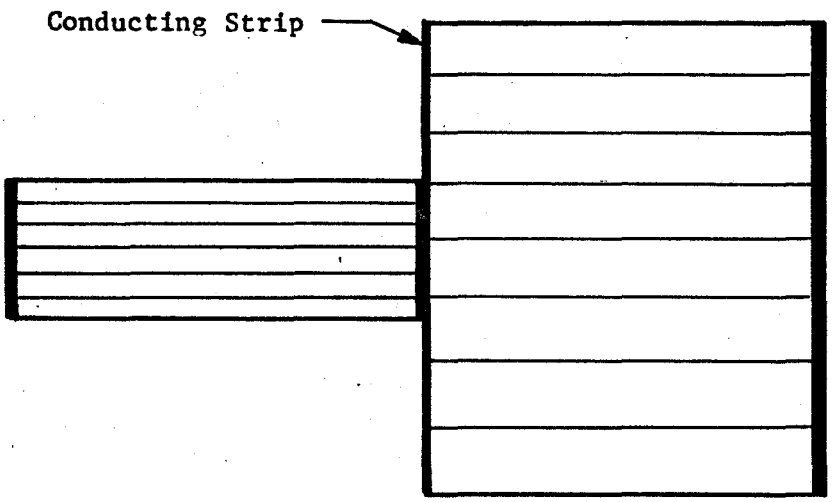

Figure 5.4

Current flow in a cascaded structure, with a conducting strip.

sentation of one-half the 4-section optimal design, is given in figure 5.5.

Eccobond solder 56c, mixed with catalyst #9, was painted in narrow strips between the sections, to simulate the necessary conducting strips. A narrow width of aluminum foil was then placed over the painted areas, to reduce the voltage drop from the centre line to the ends of the strips. This adheres well to the conducting paint, and the impedance from end to end, of a 0.2 cm. by 38.0 cm thin strip, is 0.56 ohms.

Contact pads were also painted on with the same material. But instead of aluminum foil, copper foil (0.003 inches thick) was used as the conducting material that was stuck to the conducting paint. Appropriate conducting pads are shown in figures 5.1 and 5.5.

With the insertion of conducting strips, inter-section capacitance causes complications, since the network will not respond as a strictly distributed RC network. To reduce these effects, the conducting strips and ground plane must be sufficiently separated. By fabricating the conducting strips and ground plane as in figure 5.6, these effects become negligible. Comparison of measured values (measurement of capacitance of whole structure - 680 picofarads for the ERC network) with expected values (determination of capacitance of capacitance with the knowledge of the capacitance/square and the area - 673 picofarads for the ERC network) indicates that that this assumption is valid.

To simulate as closely as possible, the thin-film structure with Mylar-Teledeltos models, it is necessary to compress the Mylar-Teledeltos-copper sheets, so that there is little or no air space between successive layers. To accomplish this, the model was sandwiched between a 3/8 inch

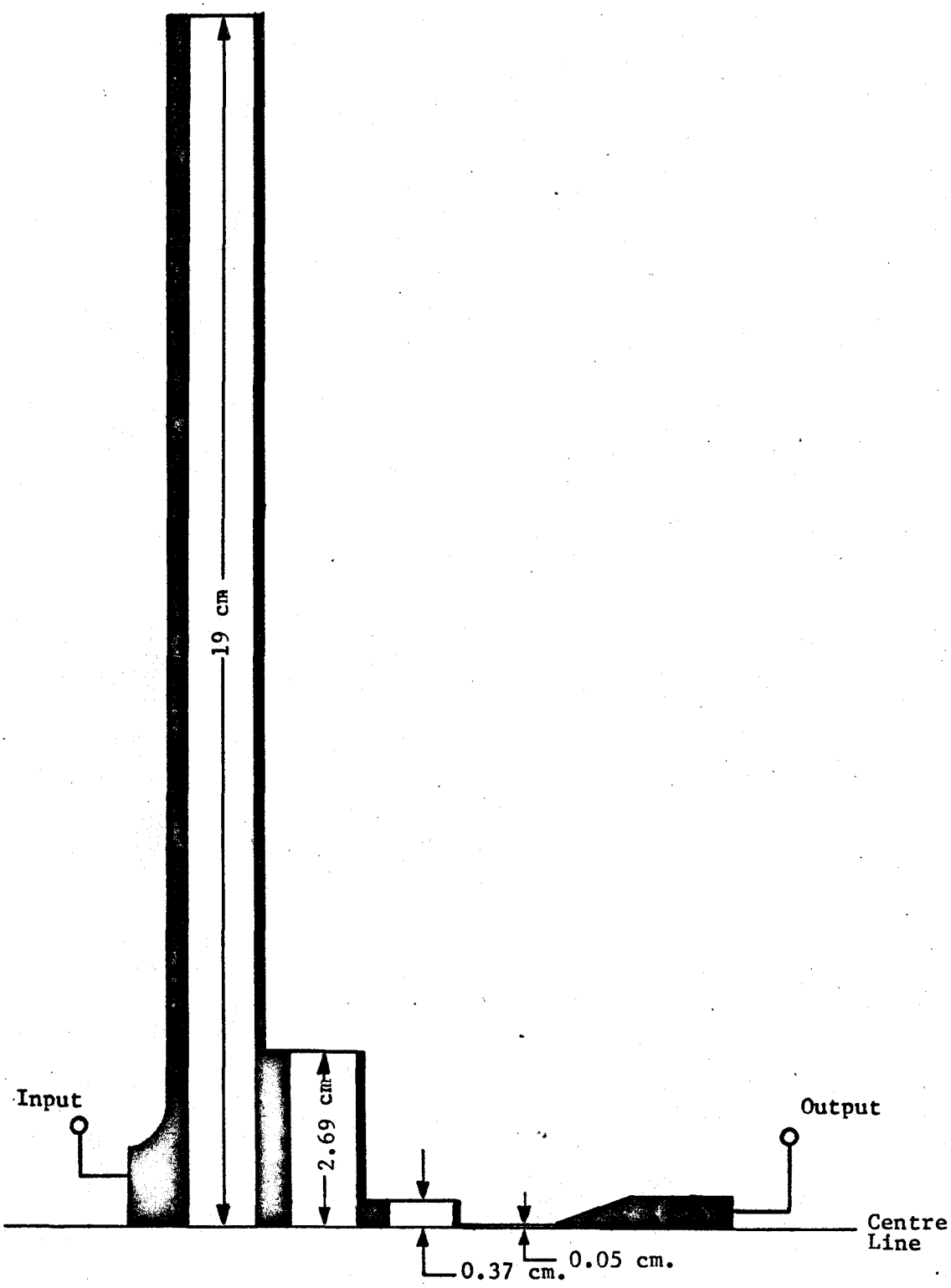

Figure 5.5

Pictorial representation of half the optimal 4-section network fabricated.

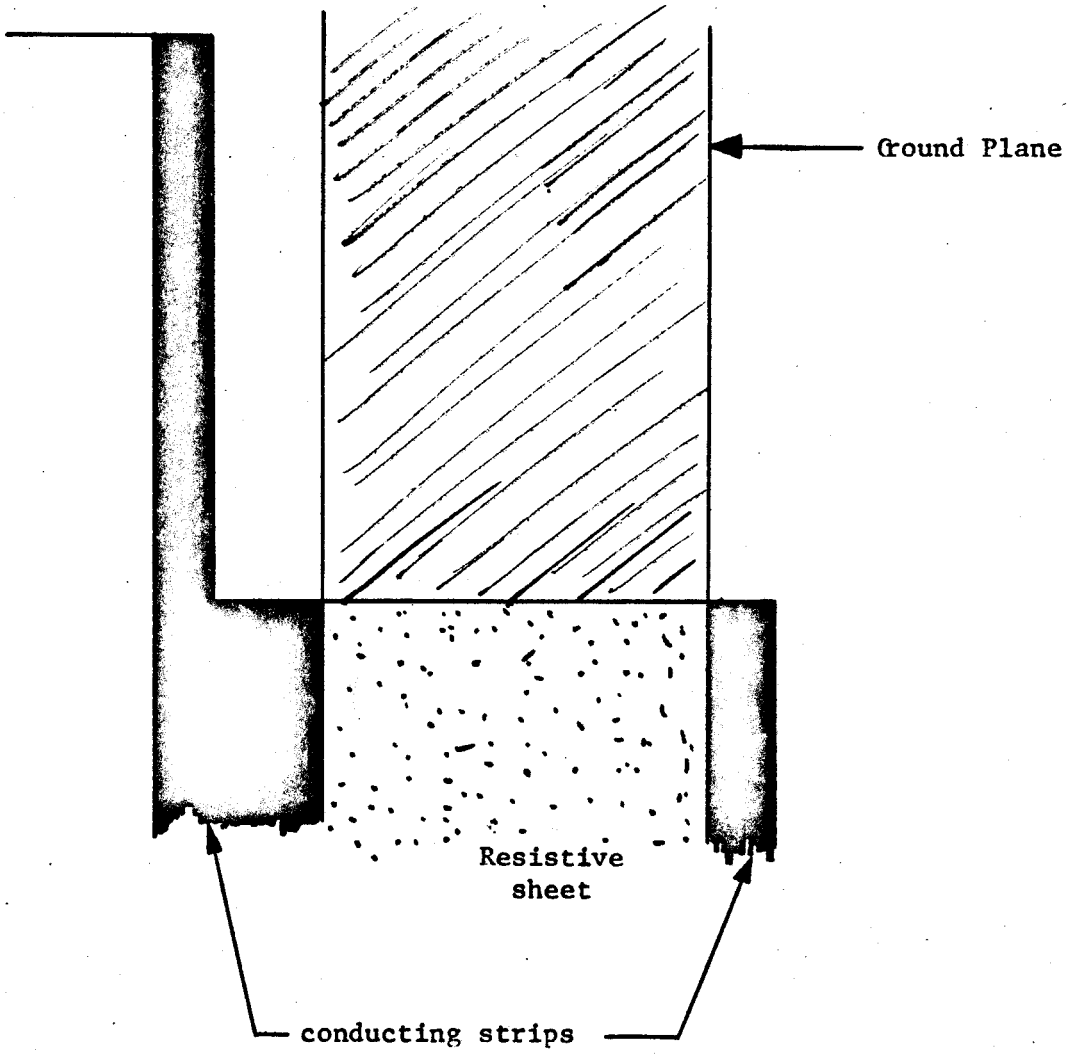

Figure 5.6

Pictorial representation of minimization of
inter-section capacitance

sheet of perspex below, and compressible pad and 1/4 inch sheet of perspex above. The compressible pad was nothing more than a household place-mat. But to maintain as much pressure as possible, over the rather large structures that were fabricated, a 60 pound weight was positioned on the 1/4 inch perspex sheet.

5.3 Experimental Results

5.3.1 Analysing Equipment

The open circuit notch filter responses were obtained by a Hewlett Packard Network Analyser. This consisted of a Hewlett-Packard 675A Sweeping Signal Generator (nominally 0.1 MHz to 32 MHz), a Hewlett-Packard 676A Phase/Amplitude Tracking Detector, a Hewlett-Packard 7562A Log Converter and a Hewlett-Packard 140A Oscilloscope. A pictorial diagram of this system is shown in figure 5.7.

5.3.2 Experimental Notch Responses

The reponses curves were obtained by photographing (with a Hewlett-Packard Model 197A Oscilloscope Polaroid Camera) the responses traced on the oscilloscope. The photographs are exhibited in figures 5.8 to 5.13. The responses to be closely examined are those of figures 5.8, 5.9 and 5.10. Figures 5.8 and 5.9 display URC and ERC (D = 1) notch filter responses, respectively. Note the improved bandwidth rejection ratio of the ERC notch network over the URC notch network, as predicted theoretically. Also, these circuits have well-documented verification in other papers.

Now contrast the response of figure 5.10 (6-section optimal de-

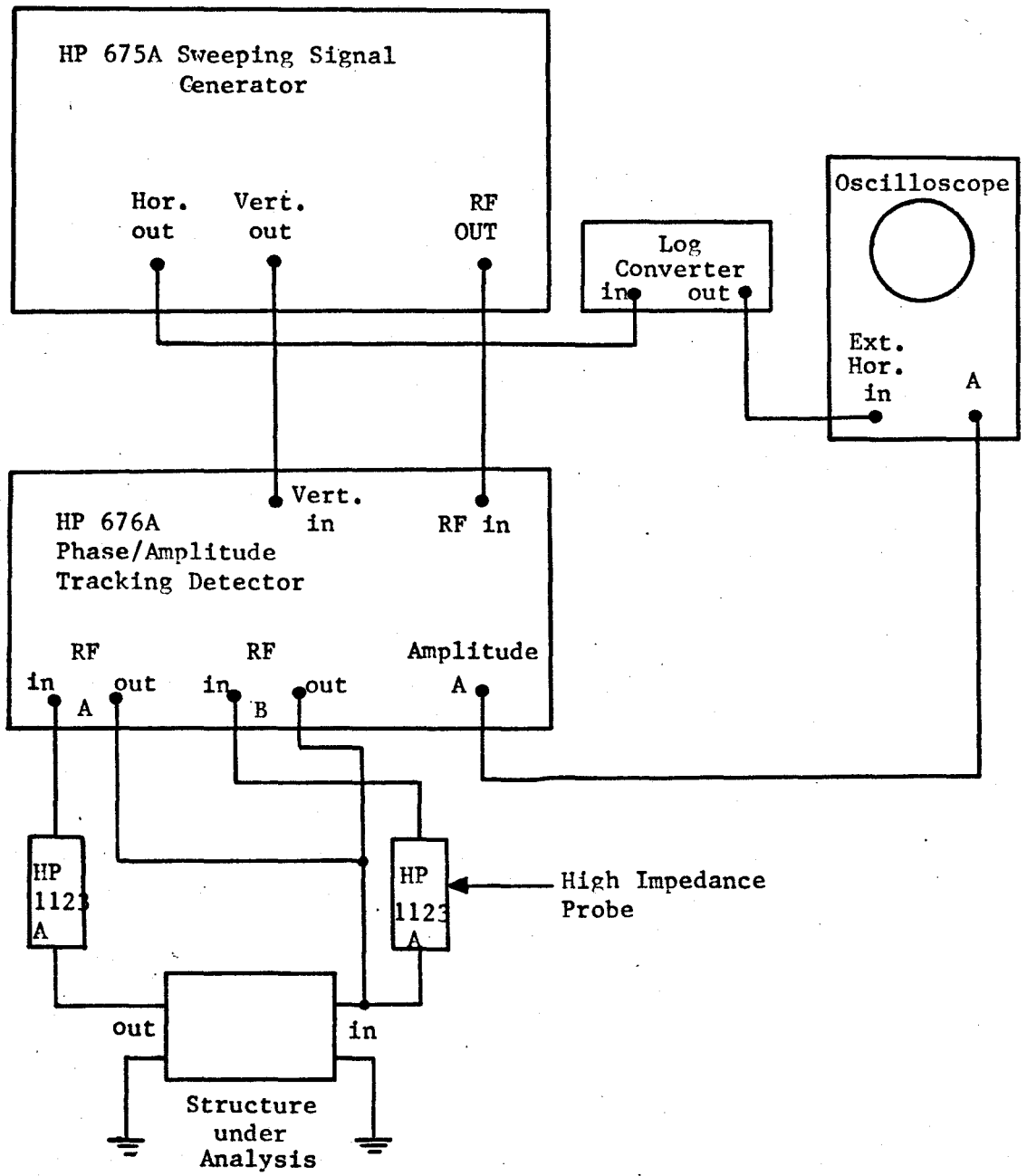

Figure 5.7

Block representation of analysing equipment to measure open circuit voltage transfer functions.

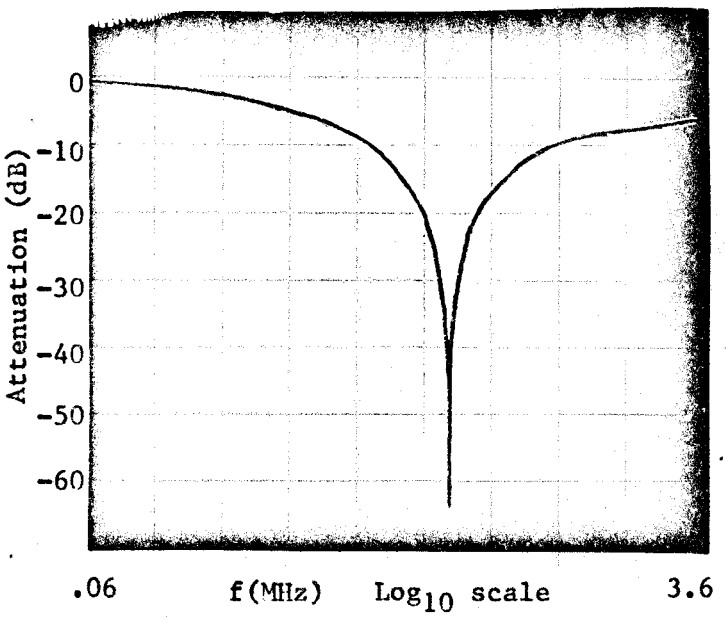

Figure 5.8

Photograph of oscilloscope trace of URC notch network response.

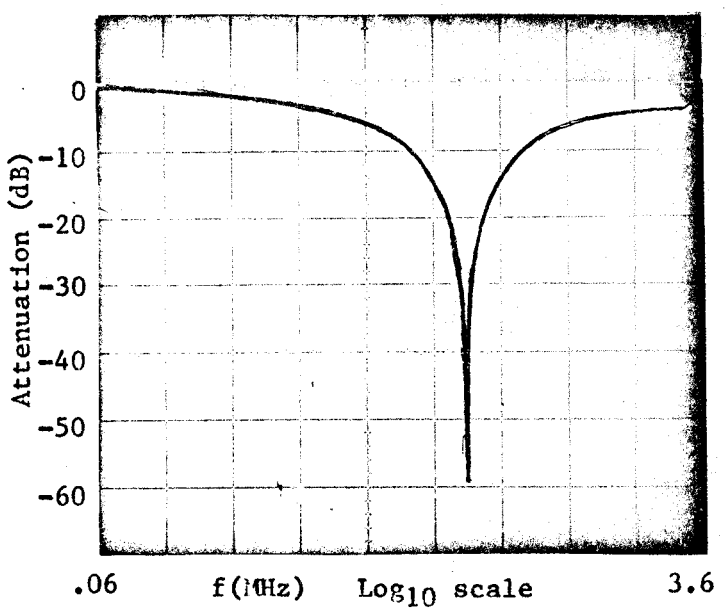

Figure 5.9

Photograph of oscilloscope trace for ERC notch network response.

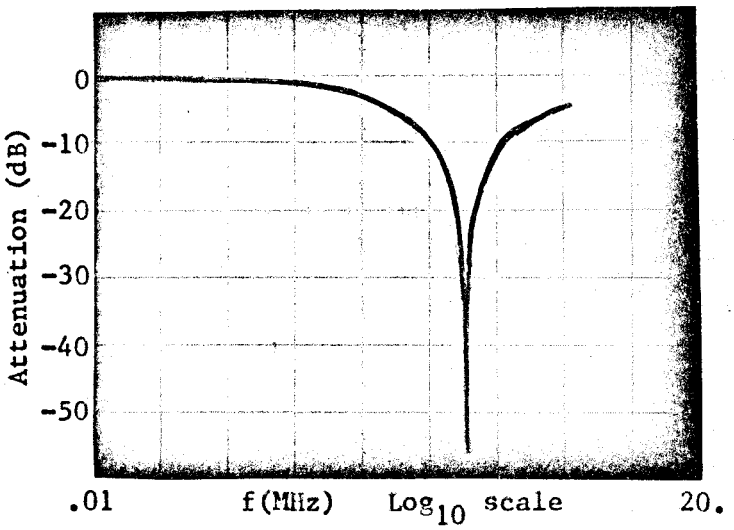

Figure 5.10

Photograph of oscilloscope trace for optimal 6-section notch network response.

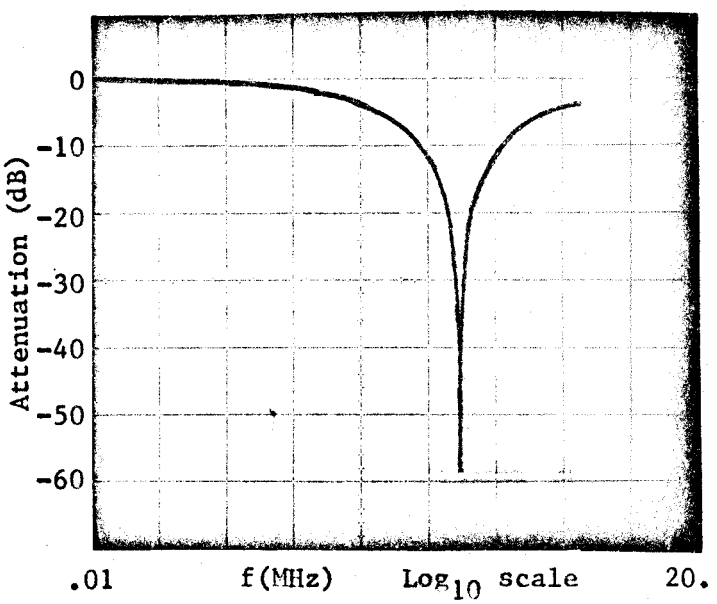

Figure 5.11

Photograph of oscilloscope trace for optimal 4-section notch network response.

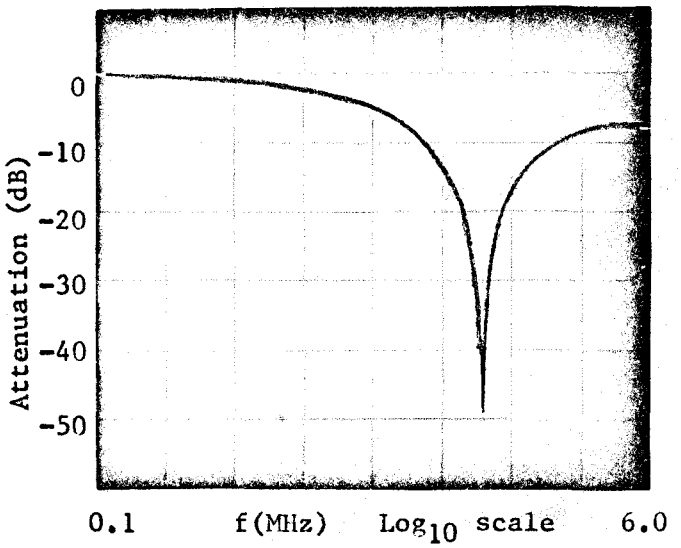

Figure 5.12

Photograph of oscilloscope trace for non-optimal 3-section notch network response.

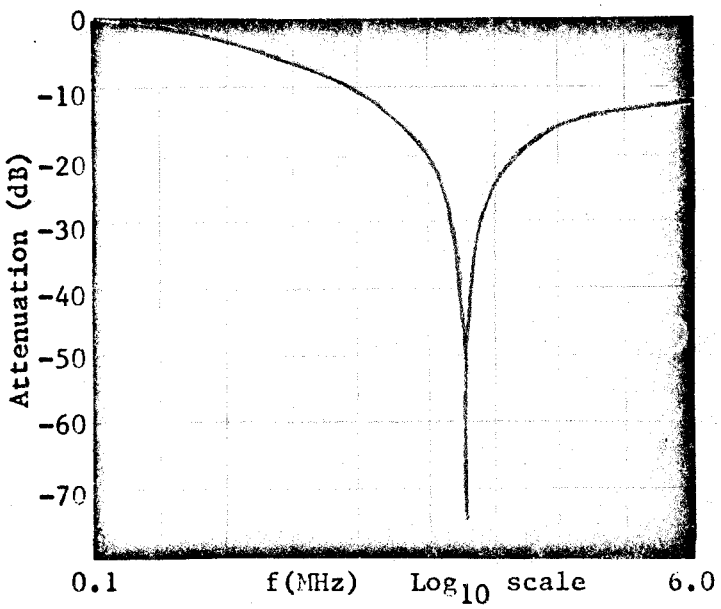

Figure 5.13

Photograph of oscilloscope trace for non-optimal 4-section notch network response.

sign) with figure 5.9 (ERC notch response). Again there is a noticeably significant improvement in the bandwidth rejection response. These improvements, in the bandwidth rejection response, are best described by collating the Q-factors of these networks.

This Q-factor is

$$Q = \frac{f_o}{\Delta f} \tag{5.1}$$

where

f_o is the notch frequency

Δf is the frequency difference, corresponding to the half-power frequencies either side of the notch. These frequen- were determined on a Hewlett-Packard 5216A Digital Frequency Counter.

The contrast of these factors is given in Table 5.1, with the highest Q attributable to the optimal 6-section network.

Table 5.1

Network	Q-factor
URC	56
ERC	93
6-section	112

Figure 5.11 is also included in this comparison, since it is the notch response of the optimal 4-section cascaded structure. It "verifies" the response shown for the 6-section network, by indicating a bandwidth rejection ratio improvement over the ERC notch network, but still not quite as improved as the 6-section notch network response.

The remaining photographs in figure 5.12 and figure 5.13, are for contrasting the optimal with non-optimal, notch network responses. Figure 5.12 is a photograph of a 3-section non-optimal design, with non-optimal widths that have been proportionally correlated, of 0.486, 0.361 and 0.072. Figure 5.13 is similarly a photograph of a response of a non-optimal cascaded network with proportionally correlated widths of 0.05, 0.12, 0.381 and 1.264 . The object of the comparisons, is to show that though the solution may yield many different configurations (using computer-aided design methods), only a test of these solutions will ascertain their reliability.

Figure 5.14 displays a comparison of the notch responses of the circuit configurations under consideration - the URC, the ERC and the optimal 6-section cascaded network. These responses were obtained by determining the attenuation from the network analyser, and reading the corresponding operating frequency from the Hewlett-Packard 5216A Digital Frequency counter. The responses exhibit similar differences as the theoretical ones of figures 4.5 and 4.7.

5.4 Experimental and Expected Results

5.4.1 Expected Values

An engineering reference data book lists the relative permittivity of Mylar polyester film, as 2.98 at 1 MHz. For a 1 square centimetre area, the expected capacitance will be 34.8 picofarads (pf). The impedance of the Teledeltos resistive layer is found as 1.83 KΩ per square. With this data, expected notch frequencies for the URC (of 4 square inch area) and the ERC (of taper D = 1, and length 10 centimeters), may be calcula-

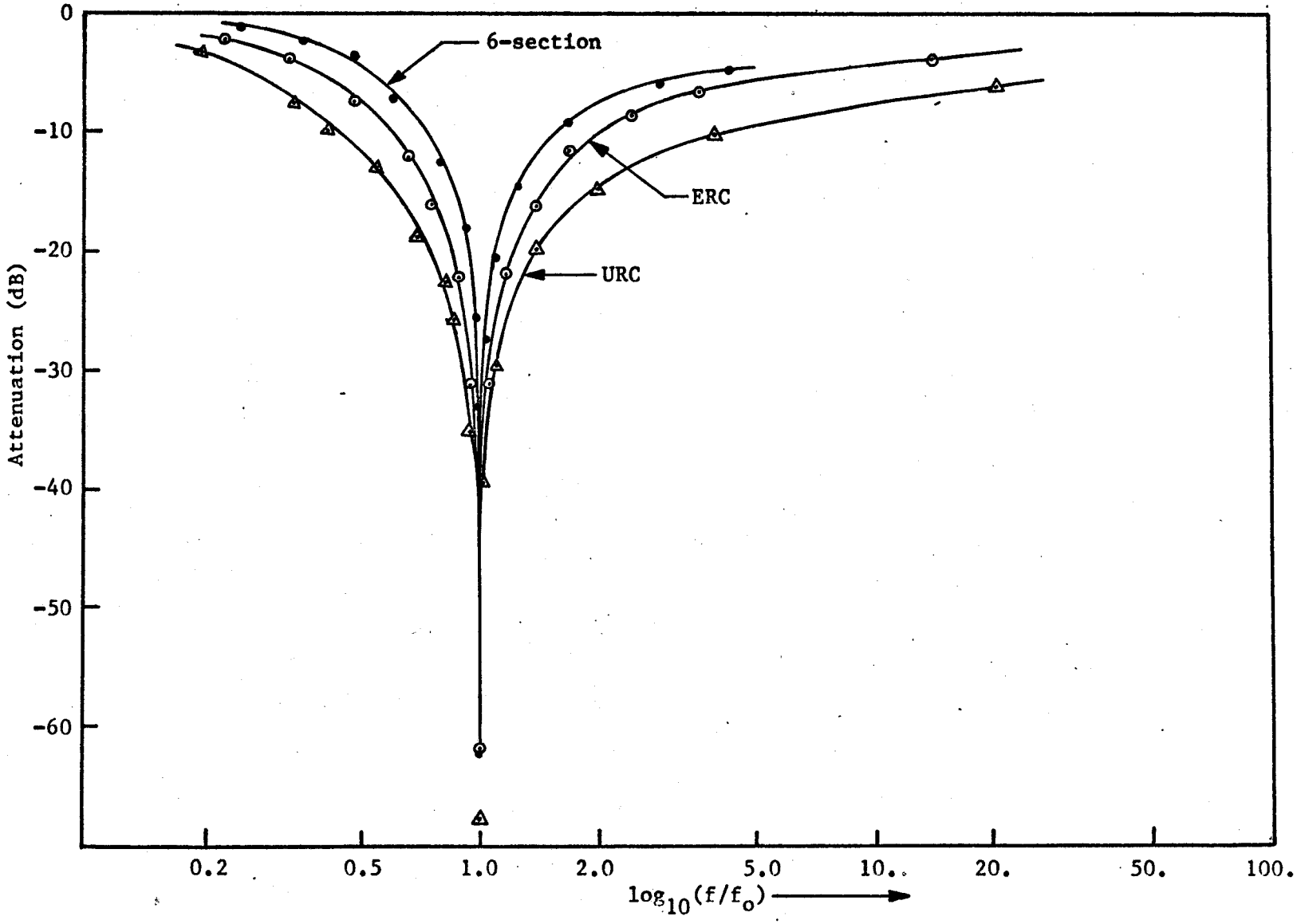

Figure 4 .14

Comparison of experimental notch responses of URC, ERC, and optimal 6-section notch networks.

ted as

$$f_o = 11.1902 \times \frac{1}{2\pi RC}$$

$$= 11.1902 \times \frac{1}{2\pi \times 1.83\times10^{3} \times 34.8\times10^{-12} \times 103.2}$$

$$= 275.5 \text{ KHz}$$

for the URC notch network. For the ERC notch network, the expected notch frequency is

$$f_o = 11.72 \times \frac{1}{2\pi RC}$$

$$= 11.72 \times \frac{1}{2\pi \times 8.76\text{-}10^{3} \times 34.9\times10^{-12} \times 26.64}$$

$$= 229.1 \text{ KHz}$$

Recall that Table 2.1 gave values of $x = \omega RC$, for the URC notch structure, at different frequency locations of the zero of transmission of the notch transfer function. Where the first null occurred, $x = 11.1902$ for the URC notch filter. A similar solution of the transfer function of the ERC notch filter will find the first null occurring for $x = 11.72$. Both of these numbers are used in the above calculations.

For the optimal 6-section design, it becomes more difficult to determine the theoretical location of the null, since there is no theoretical transfer function that may be solved. But, since the notch frequency is located with reasonable accuracy in the theoretical analysis, and the theoretical resistance and capacitance of the structure are also known

here, a reliable value for this parameter may be calculated. It is

$$x = \omega RC \qquad (5.2)$$

$$= 2\pi f_o RC$$

$$= 291.7$$

where again

f_o is the notch frequency

Hence the expected location of the notch frequency for the constructed optimal 6-section structure can be found as

$$f_o = 291.7 \times \frac{1}{2\pi RC}$$

$$= 291.7 \times \frac{1}{2\pi \times 26.9\times10^{3} \times 34.8\times10^{-12} \times 52.2}$$

$$= 0.952 \text{ MHz}$$

5.4.2 Comparison of Expected and Experimental Notch Frequencies

Table 5.2 compares the experimental notch frequencies, as obtained by the network analyser and digital frequency counter, and the expected notch frequencies as previously calculated.

From the evidence of this table, the large discrepancies must be accounted for, with reasons other than mere experimental measurement errors. Thus capacitance and losses in capacitance measurements were taken for the Mylar capacitors, and the effects these have on the notch frequency were compared.

Table 5.2

Comparison of notch frequencies

Network	Experimental notch frequency	Expected notch frequency
URC	391 KHz	275.5 KHz
ERC	326.7 KHz	229 KHz
6-section	1.23 MHz	0.952 MHz

5.4.3 Measurement of Capacitance of Mylar Model

The capacitance of the distributed network cannot be obtained by simply conecting the capacitance bridge across the input terminals of the network. Were this to be done, a measurement of the capacitance of the reactive component of the input impedance (C_r) would be obtained. That is to say

$$\text{Imag}(z_{11}) = \frac{1}{2\pi f C_r} \tag{5.3}$$

From equations (2.18 and (2.19), z_{11} may be determined, and replaced in equation (5.3). The resultant equation for C_r is

$$C_r = \frac{1}{2\pi f \ \text{Imag}(Z_o \coth \theta)} \tag{5.4}$$

If the resistive layer is then replaced with a conducting sheet, and the same structural configurations as the distributed networks, are maintained, the capacitance (C) of this lumped element can be measured as a function of frequency. It can be shown[13] that the ratio C_r/C depends only on the normalized frequency, and not on the structure

dimensions. Also, at low frequencies, the resistance of the distributed network is very small compared to the structure's reacitve capacitance. Thus the lumped capacitance measurement is a good approximation to the capacitance of the distributed network.

Capacitance measurements were performed over a range of frequencies, on a General Radio 1615A capacitance bridge. Measurements for the URC, the ERC and the optimal 6-section structure were taken, and the results obtained are given figure 5.15.

5.4.4 Losses in Mylar Capacitors

A circuit model of a non-ideal capacitor is given in figure 5.16. Carson[5] performed the analysis of the effects of leakage conductance (G) on the notch response. A parameter A is defined as

$$A = Gr_o\lambda \tag{5.5}$$

and it was demonstrated that for $A<0.1$, the effects of leakage conductance may be ignored. Since G of the URC, ERC and optimal 6-section structures is at most $<0.5\times10^{-9}$, this gives a maximum for A of less than 4.5×10^{-6}. Thus the leakage effects of the Mylar capacitor can be ignored for the purposes of this thesis.

Included in the loss analysis, are the effects of the frequency dependant series resistance $R_s(\omega)$. This resistance is related to the dissipation factor as

$$D \text{ (dissipation factor)} = \omega R_s(\omega)C \tag{5.6}$$

The dissipation factors were measured on the General Radio bridge, for

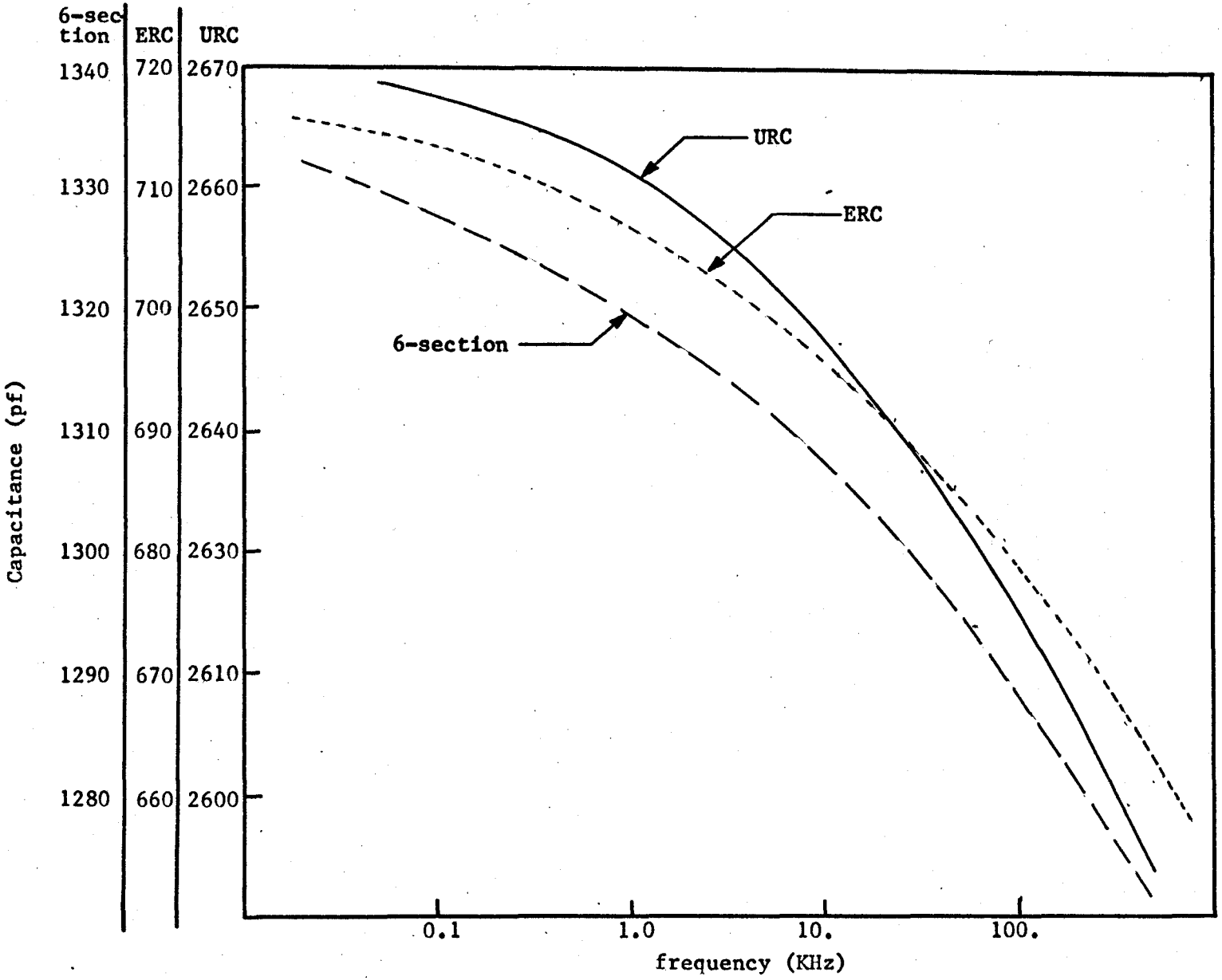

Figure 5.15

Plot of the capacitance of the URC, ERC and optimal 6-section cascaded structure.

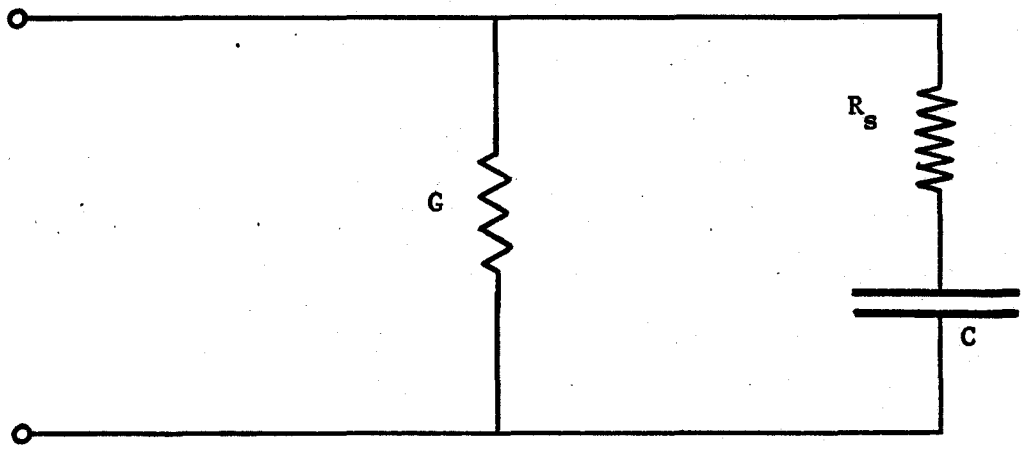

G represents the leakage conductance

C represents the capacitance

R_s represents the frequency dependent resistance, or dielectric loss

Figure 5.16

Equivalent circuit of a non-ideal capacitor

the same frequencies and networks at which the capacitance measurements were taken. The calculations, as indicated in equation (5.4), were performed, and the resultant series resistance dependancy on frequency for each network, was plotted in figures 5.17, 5.18 and 5.19.

Carson, et. al.[6], also analyse the effects of dissipation in the capacitance , on the notch frequency. A parameter B is introduced as

$$B = \frac{R_s(\omega)}{r_o \lambda} \tag{5.7}$$

At different B, the effects of $R_s(\omega)$ on the notch frequency were determined for a URC,and an ERC notch network. These effects are shown in Tables 5.3 (URC) and 5.4 (ERC).

Table 5.3

Effects of B on notch frequency parameter x, for the URC notch filter

B	x
0	11.1902
10^{-4}	11.20
10^{-3}	11.365
10^{-2}	13.7906

Table 5.4

Effects of B on notch frequency parameter x, for the ERC notch filter

B	x
0	11.72
10^{-4}	11.73
10^{-3}	11.808
10^{-2}	13.331

A similar type of analysis was performed on the optimal 6-section design, where the effects of B were incorporated in the characteristic impedance (Z_o) and the electrical length (θ). These distributed circuit parameters were reformed to,

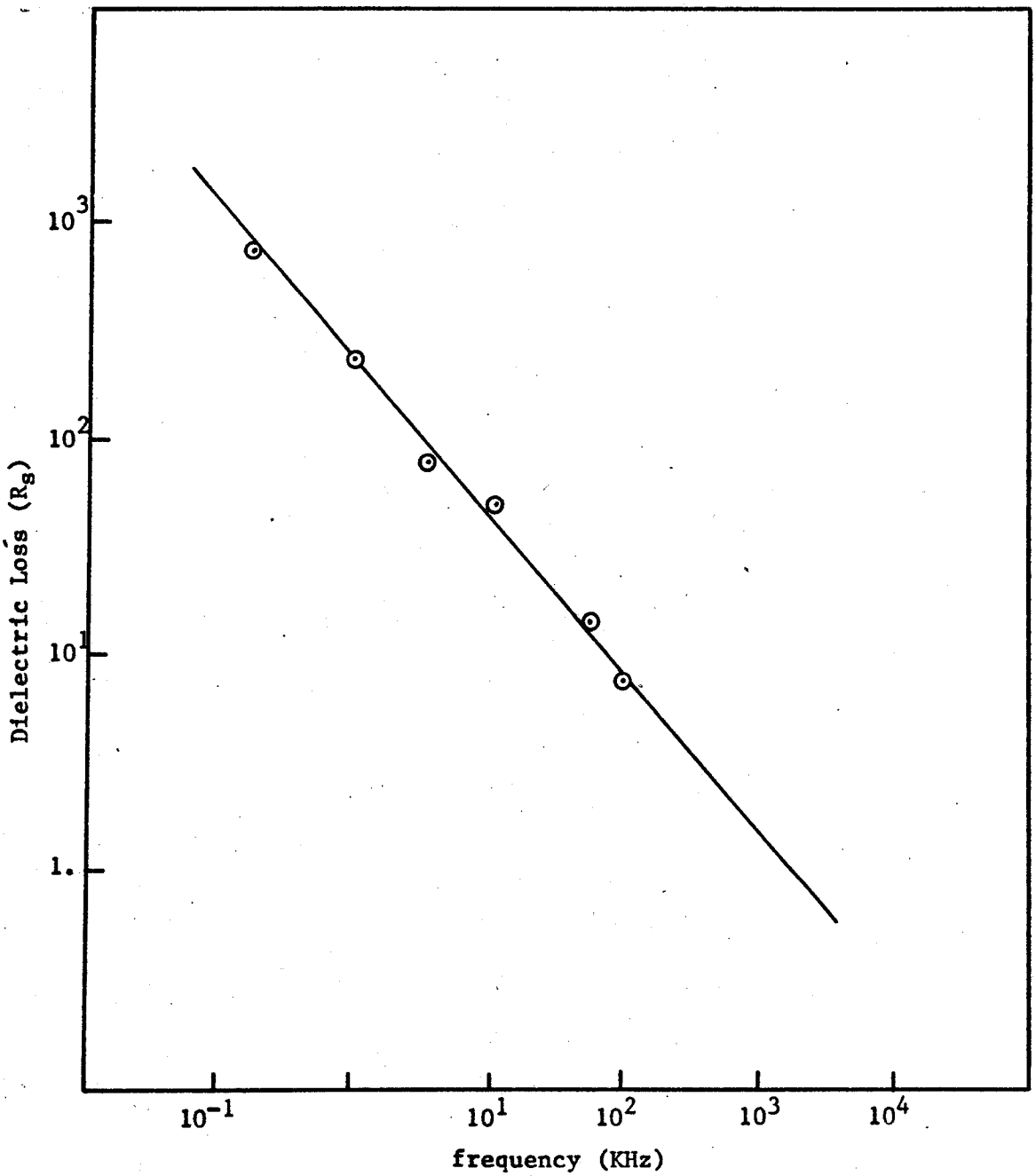

Figure 5.17

Dielectric loss of Mylar capacitor for URC structure.

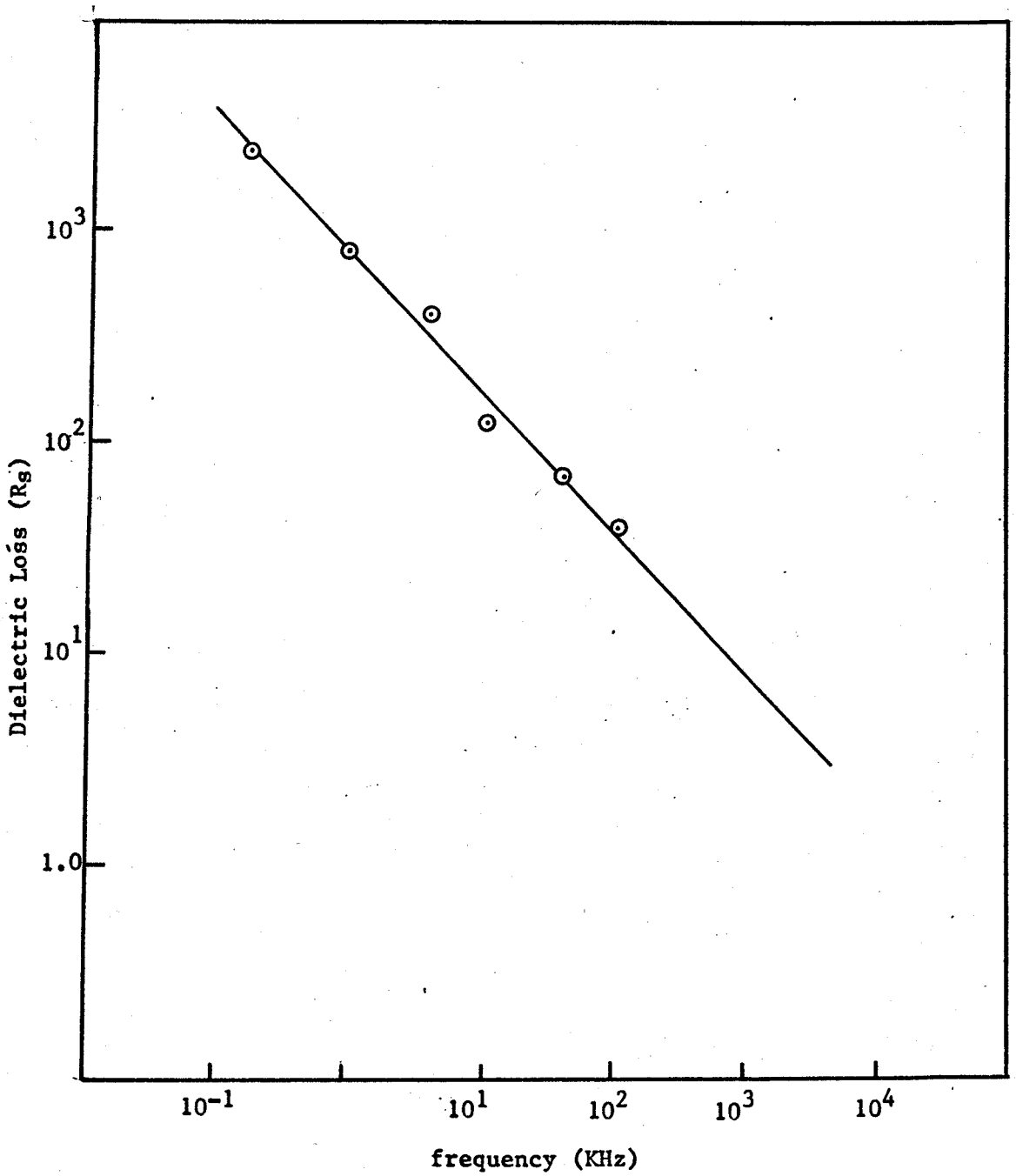

Figure 5.18

Dielectric loss for Mylar capacitor of the ERC structure.

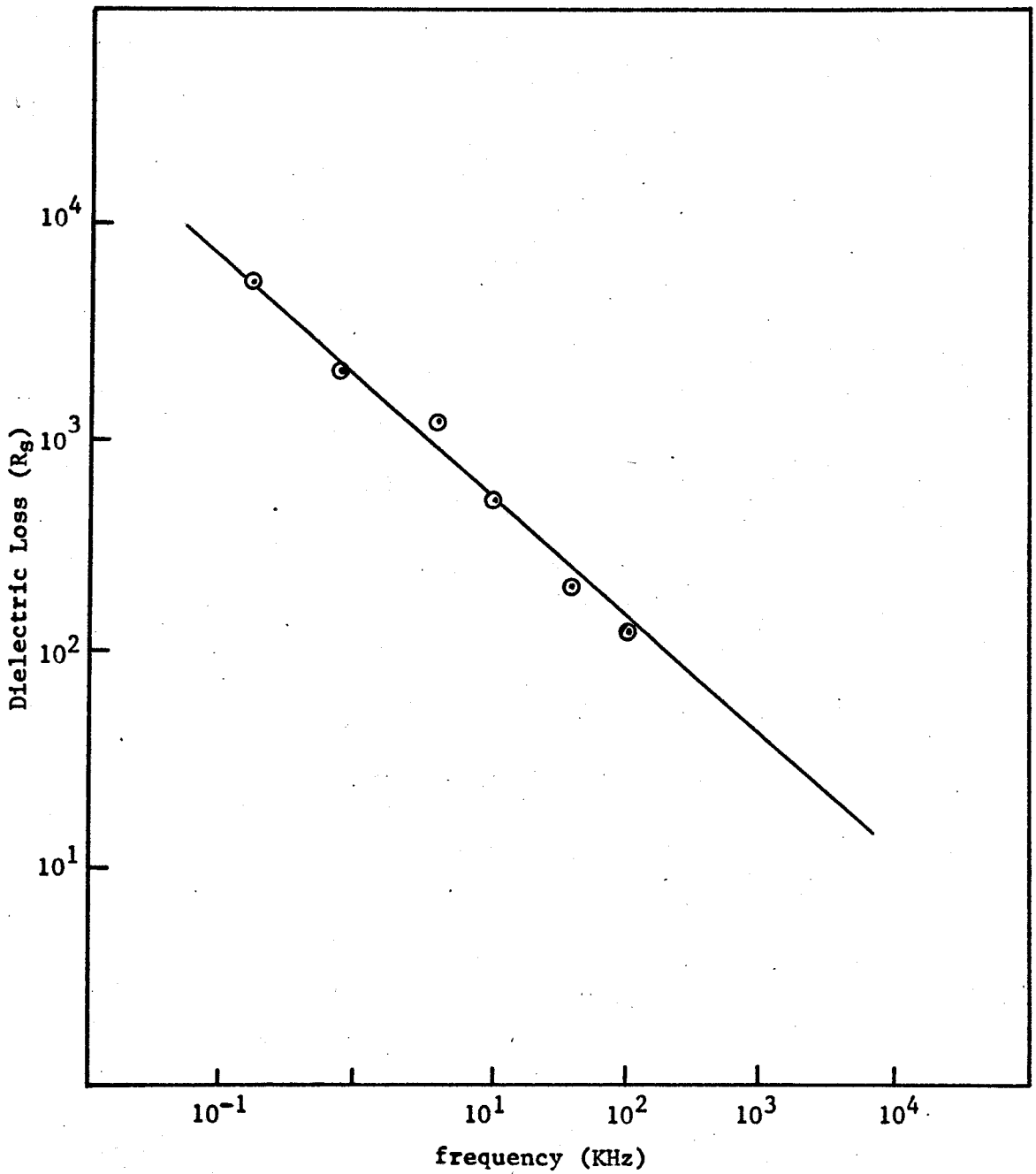

Figure 5.19

Dielectric loss of Mylar capacitor for optimal 6-section structure.

$$Z_o = \sqrt{\frac{sRC}{1 + sRCB}} \tag{5.8}$$

$$= R\sqrt{\frac{1 + sRCB}{sRC}} \tag{5.9}$$

For different values of B, the change in the location of the notch frequency of the optimal 6-section notch filter is determined. Hence the corresponding changes in the notch parameter x are also determined. The changes in x for corresponding changes in B, are given in Table 5.5.

Table 5.5

Effects of B on the notch frequency parameter x, for the optimal 6-section notch filter.

B	x
0	291.7
10^{-4}	295.2
10^{-3}	297.8
10^{-2}	309.1

5.4.5 Comparison of Experimental, Expected, and Updated Expected (which account for dissipation losses) Notch Frequency

From a measurement of the capacitance, the dissipation and the resistance of the distributed structures, it is possible to obtain the appropriate B at the notch frequency of the networks. Table 5.6 correlates the B's and the corresponding changes in x (from Tables 5.3, 5.4 and 5.5) for all the networks analysed.

Table 5.6

Changes in the notch parameter x, for the values of B determined at the notch frequency of the networks fabricated.

Network	B	x
URC	2.08×10^{-3}	11.9
ERC	2.03×10^{-3}	12.3
6-section	1.98×10^{-3}	303

With these new values for x , the corresponding changes in the expected notch frequency are compared with experimental ones in Table 5.7.

Table 5.7

Comparison of experimental, expected, and updated expected notch frequencies.

Network	Experimental notch frequency	Expected notch frequency	Updated (with losses) frequency
URC	391 KHz	275.5 KHz	290.0 KHz
ERC	326.7 KHz	229.0 KHz	241.0 KHz
6-section	1.23 MHz	0.952 MHz	0.991 MHz

But still the discrepencies between the experimental and the updated expected, notch frequencies, are too large to be discounted. Part of the solution lies in figure 6.20, which shows the changes in capacitance per square centimetre for the same pressure compressing the conducting and insulating layers.

If the capacitance of 25.3 pf per cm^2 (which is the value

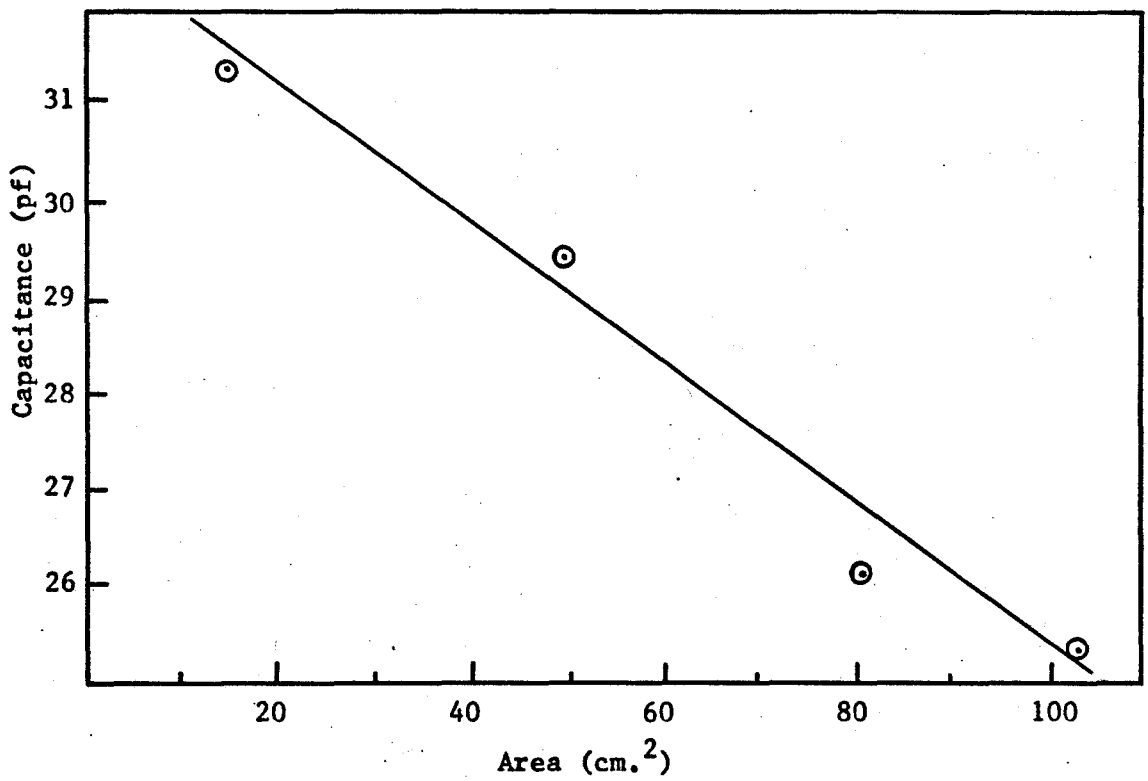

Figure 5.20

Graph to illustrate the change in capacitance of a Mylar capacitor, with variation of area of capacitor, at constant applied pressure.

obtained for the 4 square inch URC network used) were applied in the calculation of the expected notch frequency, instead of 34.8 pf per cm^2, the notch frequencies, exclusive of loss effects, would be 371 KHz 314 KHz, and 1.15 MHz, for the URC, ERC and optimal 6-section notch structures. If losses are included, these frequencies are adjusted to 394 KHz, 330 KHz and 1.195 MHz, which are more agreeable with the notch frequencies determined experimentally.

It would appear that these improved results could have been obtained, if a better type of pressure were applied, since the capacitance appears to depend on the force/unit area acting on the structure

CHAPTER 6

CONCLUSIONS AND RECOMMENDATIONS

Computer-aided design techniques were successfully applied, in obtaining the optimal shape of a thin-film RC notch filter. Although the resultant shape did not yield the originally specified response hoped for, considerable improvements over other distributed RC notch filters was obtained. It may be observed, that the greater the taper, the better one would expect the bandwidth rejection ratio to be. But physical limitations on deposited films restrict the maximum and minimum widths, as mentioned in section 3.7. Hence the optimally tapered structure, with the provision that it is contained within the proposed parameter constraints, was one which approximated an exponential of degree 3.5

In order to get any significant improvement in the notch response by increasing the degree of the exponential taper, it would become necessary to have a substrate of about 100 cm. width, so that the maximum width deposited would be 100 cm.

It can also be observed that the parameters chosen to be optimized are in fact the easiest to fabricate, when it is the optimal shape of the structure that is desired.

Note that the exponential variation need not be restricted to the 2-dimensional case. If the changes in capacitance and resistance are determined for the cascaded sections, going from input to output, it is seen that the resistance increases and the capacitance decreases, while

their product remains constant. It may also be noted that, from the ERC to the optimal 6-section structure, changes in resistance and capacitance are even more pronounced. These same effects may be obtained if the thicknesses of the resistive and capacitive layers are also varied exponentially. And possibly the next step in improving the notch response would be to vary the thickness (third dimension) of the resistive and capacitive layers. Although there would be fabrication difficulties, possibly an interface with a desk calculator, like the Hewlett-Packard 9100 A, could control the shutter speed as it traversed the length of the structure.

Conclusively, the experimental results bear out the theoretical predictions, as long as calculations for capacitor losses are considered, and the effects of pressure and size of the structures are accounted for. Hence Mylar-Teledeltos can justifiably replace thin-film distributed circuits, if size and pressure considerations are included.

REFERENCES

1. Bandler, J. W. , "Optimization Methods for Computer-Aided Design", IEEE Trans. on Microwave Theory and Techniques, Vol. MTT-17, Aug. 1969, pp 533 - 552.

2. Bandler, J. W., and Charalambous, C., "Theory of Generalized Least p^{th} Approximation, IEEE Trans. on Circuit Theory, Vol. CT-19, May 1972, pp 287 - 289.

3. Bandler, J. W., and Seviora, R. E., "Current Trends in Network Optimization", IEEE Trans. on Microwave Theory and Techniques, Vol MTT-18, Dec. 1970, pp 1159 - 1170.

4. Campbell, C. K., "Transmission Line Graphical Analysis of Distributed RC Notch Filters", IEEE Vol. No. 9, Sept. 1971, pp 1362 - 1363.

5. Carson, J. A., "Evapourated Thin-Film Distributed RC Networks", Master's Thesis, McMaster University, Hamilton Ontario. Dec 1969.

6. Carson, J. A., Campbell, C. K., Swart, P. L., and Vallo, F. J., Effects of Dielectric Losses on the Performance of Evapourated Thin-Film Distributed RC Notch Filters", IEEE Solid-State Circuits Vol SC-6, June 1971, pp 120 - 124.

7. Director, S. W., and Rohrer, R. A., "The Generalized Adjoint Network and Network Sensitivities", IEEE Trans. on Circuit Theory, Vol. CT-16, Aug. 1969, pp 318 - 323.

8. Feynman, R. P., Leighton, R. B., and Sands, M., "The Feynman Lecture Series on Physics" Vol. II, Addison-Wesley Publishing Co. Incorporated, 1964.

9. Fletcher, R, and Powell, M. J. D., "A Rapidly Convergent Descent Method for Minimization", Computer Journal, Vol. 6, pp 163 - 168, June 1963.

10. Chaussi, M. S., and Kelly, J. J., "Introduction to Distributed Parameter Networks", Holt, Rhinehart and Winston, 1968.

11. Heizer, K. W., "Distributed RC Networks With Rational Transfer Functions", IEEE Trans. on Circuit Theory, Vol. CT-9, pp 356 - 362.

12. Howard W. Sams and Co. Incorporated, "Reference Data for Radio Engineers".

13. Johnston, W. R. E., "The Use of Distributed Parameter Networks as Feedback Elements", Master's Thesis, McMaster University, Hamilton Ontario, April 1972.

14. Kaufman, W. M., "Theory of Monolithic Null Devices and Some Novel Circuits", Proc. IRE 48, 1960, pp 1540 - 1545.

15. Kaufman, W. M., and Garret, S. J., "Tapered Distributed Filters", IRE Trans. on Circuit Theory, Vol. CT-9, Dec. 1962, pp 329 - 336.

16. Kelly, J. J., and Ghausi, M. S., "Tapered Distributed RC Networks With Similar Immittances", IEEE Trans. on Circuit Theory, Vol. CT-12, Dec. 1965, pp 554 - 558.

17. Lee, S. C., and Penbeci S. S., "Computer-Aided Design of Distributed RC Networks", IEEE Trans. on Circuit Theory, Vol. CT-17, Aug. 1969, pp 224 - 232.

18. Morse, P. M., amd Feshback, H.,"Methods of Theoretical Physics", McGraw-Hill Book Co., 1963.

19. Oehler, K. L., "Analysis and Synthesis of Distributed Parameter Circuits", Ph. D. Thesis, University of Texas, 1964.

20. O'Shea, R. P., "Synthesis Using Distributed RC Networks", 1965 Convention Records, Vol. 13, p. 7, pp 18 - 29.

21. Pierre, D. A., "Optimization Theory With Applications", John Wiley and Sons Inc., 1969.

22. Protonotarios, E. N., and Wing, O., "Theory of Nonuniform RC Lines", IEEE Trans. on Circuit Theory. Vol. CT-14, March 1967, pp 2 - 12.

23. Sokolnikolf, I. S., and Redheffer, R. M., "Mathematics of Physics and Modern Engineering, McGraw-Hill, 1966.

24. Stein, J., "A New Look at Distributed RC Notch Filters", Proc. IEEE 58, 1970, pp 596.

25. Swart, P. L., "Evapourated Thin-Film Tunable Distributed RC Filters" Ph. D. Thesis, McMaster University, Hamilton Ontario, 1971.

26. Swart, P. L., and Campbell , C. K., "Effects of Inductance on Characteristics of A Distributed RC Notch Filter", No. 9, Sept. 1971, pp 1371 - 1373.

27. Walsh, E. D., and Close, C. M., "On Synthesis of Any RC-Realizable Rational Transfer Function, Using Nonuniform Distributed RC Circuits", IEEE Trans on Circuit Theory, Vol. CT-17, May 1970, pp 217 - 223.

28. Wilson, B. L. H., and Wilson, R. B., "Shaping of Distributed RC Networks", Proc. IRE (Correspondence), Vol. 49, Aug. 1961, pp 1330 - 1331.

29. Wyndrum Jr., R. W., "The Exact Synthesis of Distributed Parameter RC Ne-works", Ph. D. dissertation , New Nork University, May 1963.